Multiaccess Performance Optimization Via Joint Phase and Polarization Beamforming

Srishti Sharma and Swades De

***Abstract*—This paper studies the performance improvement of a multi-user downlink system via polarization design at the transmitter such that the gains at the desired locations are maximized. To this end, a weighted sum rate maximization problem is formulated, constrained under total power, polarization norm, and a minimum signal-to-interference-and-noise ratio guarantee to the users for simultaneous transmission (ST), and its performance is compared with time-shared transmission (TT). As a solution strategy, weighted minimum mean square error based and fair resource allocation algorithms have been proposed to optimize ST and TT respectively with only long-term channel statistics as well as with channel state information (CSI) at the transmitter. Weighted sum rate performance is theoretically studied for long-term channel statistics. Branch-and-bound approach and the duality gap are considered to validate the optimal resource allocation with CSI for small-scale and large scale scenarios, respectively. Simulation results show that the proposed joint phase and polarization beamforming consistently enhances the multiaccess performance with respect to only phase beamforming, with average gain of about 23% and 6% with CSI and 89% and 4% with long-term channel statistics for ST and TT, respectively. We also study the performance of the proposed beamforming strategies with imperfect CSI and non-orthogonal multiple access-based ST to capture practical scenarios.**

***Index Terms*—Joint beamforming, weighted minimum mean square error (WMMSE), simultaneous transmission, time-shared transmission, dual polarization, channel state information (CSI)**

I. Introduction

The increasing demand for higher data rates and improved spectral efficiency in wireless communications has driven significant research on efficient multiaccess strategies. Several orthogonal and non-orthogonal multiaccess schemes and their combinations have been developed with the common objective of interference mitigation and spectral efficiency optimization [1], [2]. Many of these approaches rely on manipulating fundamental properties of electromagnetic (EM) waves, such as time, frequency, and spatial dimensions, as well as transmitter- or receiver-side signal processing techniques like beamforming and interference cancellation (IC) [3], [4], [5].

Beamforming technology in particular has played a central role in improving the performance of multi-user systems employing multiple antennas such as time division multiple access (TDMA), space division multiple access (SDMA), non-orthogonal multiple access (NOMA), rate-splitting multiple access (RSMA), and multi-user multiple input multiple output (MIMO) [4], [6], [7], [8]. Several precoding strategies have been proposed that optimize signal power and phase to manage interference [9], [10]. However, an inherent property of EM waves, polarization has been relatively underutilized despite offering an additional gain in the signal space which can be leveraged to improve the system performance.

Recent advancements have shown that polarization can enhance communication through modulation [11], [12], multiplexing [13], and diversity techniques [14], [15]. Moreover, dual-polarized antenna systems are increasingly used in multiple antenna setups to reduce spatial correlation and pack more antennas into limited physical space [16].

A. Literature Review and Motivation

Growing realization on the importance of polarization has prompted the integration of polarization-based techniques in wireless communications. Recent studies have explored dual-polarized channel estimation [17], phase beamforming in dual-polarized systems [18], and RIS-aided dual-polarized systems [19], [20]. Polarization has also been applied in spatial modulation [11], spatial multiplexing [21], and channel modeling [22], [23], [24]. Interest in dual-polarized systems is driven by the inherent orthogonality of polarization. When combined with other transmission modes, this polarization orthogonality can be extended to support multi-user systems, making it highly attractive for next generation communications.

Several works have considered polarization in multi-user systems to achieve near optimal performance through low complexity beamforming techniques. The performance of these approaches hinge on the accuracy and timeliness of channel state information (CSI). The research in [25] compares the performance of classical linear precoders such as minimum mean square error (MMSE), zero forcing (ZF) and maximal ratio (MR) in dual-polarized multi-user system under perfect CSI. Others, such as [26], investigate dual-polarized RSMA with CSI estimation in every coherence interval, under imperfect IC. Limited feedback hybrid beamforming with practical antenna radiation pattern is considered in [27]. The researchers in [28], [29] demonstrated the ability of polarization-division multiple access in serving two users simultaneously by adjusting transmitter or receiver parameters.

Though CSI availability increases accuracy, it is computationally expensive and quickly becomes outdated in high mobility scenarios, thus degrading the performance. For reduced complexity in dynamic environments, precoding designs under long-term statistics proposed in [8], [30] showed promising performance under polarization multiplexing and diversity. The impact of imperfect CSI has been addressed through regularized ZF and signal to leakage and noise ratio based precoding strategies [31], [32]. Dual structured linear precoding for

The authors are with the Department of Electrical Engineering and Bharti School of Telecommunication, Indian Institute of Technology Delhi, New Delhi, India (e-mail: {Srishti.Sharma, swadesd}@ee.iitd.ac.in).

dual polarization multi-user secure communication has been proposed in [33] with both perfect and imperfect CSI. The above-cited works show that beamforming has been employed in performance enhancement of various dual-polarized communication systems. However, these beamforming techniques do not utilize all the possible states of polarization; instead they restrict to certain scenarios of power and phase relation between the polarization basis. *Moreover, these techniques do not discuss the optimal state of polarization for transmission.*

The work in [34] aimed spectral efficiency maximization via polarization optimization, however the analysis considered only linear polarization. Hybrid polarized beamforming optimization was proposed in [35], where the total transmit power is equally divided among the users. To mitigate channel depolarization, in [36] power allocation across two orthogonal polarization components was studied in a single-user scenario. We note that, the existing works did not jointly optimize transmit power, phase, and polarization in a multi-user system; they often impose simplifying assumptions on the polarization state or do not ensure minimum rate guarantees. Some works considered minimum rate constraints for sum rate maximization, but only in single-polarization systems [37], [38]. To this end, we argue that detailed study on polarization-aware communication is crucial as it enables improved quality of service in user-specific channel conditions, including orientation mismatch and mobility scenarios.

Recognizing the increasing relevance of polarization in communication systems, this work explores joint optimization of polarization along with phase in the broader context of multiaccess. *In this work, polarization beamforming along with phase beamforming is termed as joint beamforming.* The proposed joint beamforming design in multi-user downlink scenario aims to maximize the weighted sum rate subject to transmit power, polarization stability (i.e., unit polarization norm), and minimum signal-to-interference-and-noise ratio (SINR) constraints. The performance is analyzed in a simultaneous transmission (ST) while using a time-shared transmission (TT) as a benchmark as it captures no interference scenario. The iterative weighted MMSE (WMMSE) precoder is used to maximize the sum rate for ST [39]. The proposed approach complements the study in [40] which did not consider the effect of polarization in WMMSE-based sum rate maximization. The joint beamforming performance is compared with phase beamforming for ST and TT. *We emphasize that the proposed joint beamforming method is general and can be employed in other multiaccess strategies.*

B. Contributions and Significance

The inclusion of polarization increases the dimensionality of the problem due to the consideration of dual-polarized channel model which involves the product of complex matrices. Keeping these aspects in mind, the following contributions are made through this work.

1) We analyze the multiaccess performance through joint beamforming and capture the gain with respect to only phase beamforming, thereby highlighting the benefits of effectively using the signal polarization in beamforming.
2) The proposition of joint beamforming is investigated in multi-user system with dual-polarized antennas at the base station and users for ST and TT scenarios. To analyze the performance, beamforming matrices for the two strategies are designed and the weighted sum rate maximization problem is formulated for ST and TT.
3) We integrate the polarization aspects in the classical WMMSE framework and formulate the CSI-based and long-term channel statistics based iterative approaches for maximizing the weighted sum rate performance for ST under total power, polarization norm, and SINR guarantee constraints. We derive polarization-integrated MMSE receive filter and user weights considering dual-polarized channel model and formulate alternating optimization problem for iteratively computing beamformers and optimal power distribution. For a fair comparative study of ST and TT performance, a resource allocation algorithm is proposed to solve the optimization formulated for TT.
4) The SINR constraint is convexified using polarization-integrated second-order cone programming (SOCP) and an approximate SOCP constraint is considered under long-term channel statistics. A rate-based iterative approach for weight optimization is used to maintain fairness among the users. Performance is studied under varying channel conditions and system configurations.
5) Closed-form expressions of the system performance are derived in terms of Rician K factors, channel cross-polarization discrimination (XPD), and optimal phase, polarization, and power. The expression for WMMSE-based average weighted sum rates in ST and upper bound for TT are provided in terms of channel parameters. Computational complexity of the proposed algorithms for ST and TT are computed.
6) To capture real environmental scenarios, the proposed beamforming strategies are analyzed with ST for two cases: (i) impact of imperfect CSI and (ii) impact of joint beamforming on NOMA performance.

We further emphasize that the joint beamforming is particularly important in multiaccess systems, where efficient interference management and scalable user support are critical. Consequently, joint beamforming is a key enabling technique for realizing the full potential of dual-polarized systems in contemporary and future wireless communication networks.

Remark 1. *To the best of our knowledge, this is the first work that jointly optimizes polarization and phase beamforming in a multi-user system with user-specific SINR guarantee, thereby advancing polarization-aided multiaccess design.*

C. Paper Organization

The paper is organized as follows. Section II presents the wireless system configuration for studying the impact of joint beamforming. In Section III, weighted sum rate maximization problem is formulated under ST and WMMSE-based algorithms are proposed. The weighted sum rate maximization problem under TT is formulated in Section IV and algorithms are proposed to solve it. Performance results are presented in Section V, followed by the concluding remarks in Section VI.

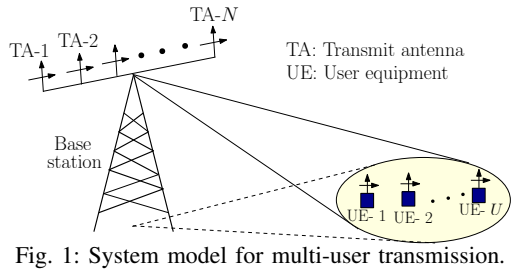

Fig. 1: System model for multi-user transmission.

II. System Model with Dual-Polarized Antennas

A. System Configuration

We consider downlink multi-user data transmission in a multi antenna system composed of one base station and U users. The base station is equipped with uniform linear array of N dual-polarized antennas and each user is equipped with a single dual-polarized antenna. Each dual-polarized antenna is composed of collocated horizontal and vertical polarized components. Polarization design is achieved by controlling the effective polarization formed at each antenna by means of dual-polarized antenna. Polarization vector of the n^{th} transmitter antenna and u^{th} receiver antenna can be written as $\mathbf{t}_n \in \mathbb{C}^{2\times 1}$ and $\mathbf{q}_u \in \mathbb{C}^{2\times 1}$, respectively. We analyze the user performance under two different conditions: (a) *CSI available at the transmitter*: resource allocation is based on instantaneous channel estimation which is performed in every coherence interval, (b) *Long-term channel statistics at the transmitter*: resource optimization is based on the channel statistics such as mean and variance. Table I lists the key notations and symbols used in this work.

B. Channel Model

In this work, we model dual-polarized channel as a Rician fading channel which is composed of a constant component and a random component, and the overall channel gain is

$$\mathbf{H} = \sqrt{\frac{K}{K+1}}\tilde{\mathbf{H}} + \sqrt{\frac{1}{K+1}}\hat{\mathbf{H}} \tag{1}$$

where K is the Rician K-factor and the gain matrix $\mathbf{H}$ is

$$\mathbf{H} = \begin{bmatrix} [\mathbf{H}_{11}] & [\mathbf{H}_{12}] & \cdots & [\mathbf{H}_{1N}] \\ [\mathbf{H}_{21}] & [\mathbf{H}_{22}] & \cdots & [\mathbf{H}_{2N}] \\ . & . & \cdots & . \\ [\mathbf{H}_{U1}] & [\mathbf{H}_{U2}] & \cdots & [\mathbf{H}_{UN}] \end{bmatrix} \in \mathbb{C}^{2U\times 2N}. \tag{2}$$

$\tilde{\mathbf{H}}$ and $\hat{\mathbf{H}}$ represent the line of sight (LOS) and the non-LOS (NLOS) components. In (2), $\mathbf{H}_{un} = [h_{un}^{hh}, h_{un}^{hv}; h_{un}^{vh}, h_{un}^{vv}]$, $u \in \mathscr{S}_1$, $n \in \mathscr{S}_2$ is a block matrix denoting the link between n^{th} transmitter antenna and u^{th} user antenna describing the relation between co-polarized and cross-polarized components.

During wireless propagation, signal undergoes reflection, refraction, diffraction, and scattering leading to cross-polarization leakage, which changes the polarization of the EM wave at the receiver. This polarization alteration ability of the wireless channel on propagation is termed as XPD. XPD phenomenon only causes exchange of energy between the two orthogonal polarization and does not cause any loss of energy from or within the channel. As XPD is the fast fading part of the channel, we consider it to be independent of the transmitter antenna element. Keeping energy conservation principle in mind, we define XPD for the LOS and NLOS path between transmitter and u-th receiver as [25]

$$\text{XPD}_{Lu} = \frac{\mathbb{E}\{|\tilde{h}_u^{hh}|^2\}}{\mathbb{E}\{|\tilde{h}_u^{vh}|^2\}} = \frac{\mathbb{E}\{|\tilde{h}_u^{vv}|^2\}}{\mathbb{E}\{|\tilde{h}_u^{hv}|^2\}} = \frac{1-\alpha_{Lu}}{\alpha_{Lu}} \tag{3}$$

$$\text{XPD}_{Nu} = \frac{\mathbb{E}\{|\hat{h}_u^{hh}|^2\}}{\mathbb{E}\{|\hat{h}_u^{vh}|^2\}} = \frac{\mathbb{E}\{|\hat{h}_u^{vv}|^2\}}{\mathbb{E}\{|\hat{h}_u^{hv}|^2\}} = \frac{1-\alpha_{Nu}}{\alpha_{Nu}} \tag{4}$$

with $0 \le \alpha_{Lu}, \alpha_{Nu} \le 1$. Symmetric leakage for horizontal and vertical polarization is assumed [23].

Next, based on XPD, we define constant and random components of the channel. LOS channel between the n^{th} transmitter and u^{th} receiver, $\tilde{\mathbf{H}}_{un}$, if present, can only be impacted by the channel XPD and can be expressed as

$$\tilde{\mathbf{H}}_{un} = \tilde{\mathbf{X}}_u = \begin{bmatrix} \sqrt{1-\alpha_{Lu}} & \sqrt{\alpha_{Lu}} \\ \sqrt{\alpha_{Lu}} & \sqrt{1-\alpha_{Lu}} \end{bmatrix}. \tag{5}$$

Using the Kronecker model, NLOS channel between n^{th} transmitter and u^{th} receiver, incorporating channel XPD is

$$\hat{\mathbf{H}}_{un} = \hat{\mathbf{X}}_u \odot \mathbf{G}_{un} \tag{6}$$

TABLE I: Notations and symbols

Parameter	Description
$(\cdot)^T$, $(\cdot)^H$	Transpose, conjugate transpose
$\lvert\cdot\rvert, \lvert\lvert\cdot\rvert\rvert$	Absolute value and Frobenius norm
$\otimes$, $\odot$	Kronecker product, Hadamard product
$\mathbf{1}_{U\times N}$	$U \times N$ matrix with every element 1
$\mathbf{0}$	Zero matrix
$\mathbb{E}[\cdot]$, $\forall$, $\in$	Expectation operator, for all, belongs to
$\mathbb{R}$, $\mathbb{C}$	Set of real and complex numbers
$\mathscr{N}(\mu, \sigma^2)$	Normal Distribution; parameters μ & σ^2
P_t, K	Transmit power, Rician K Factor
$\mathbf{t}_n$	Polarization vector of n^{th} transmitter
$\mathbf{q}_u$	Polarization vector of u^{th} receiver
$\tilde{\mathbf{H}}$, $\hat{\mathbf{H}}$	LOS and NLOS channel matrix
$\kappa_{mn,u}^w$	Transmit correlation (m,n) for user u
$\varrho_{ul,n}^w$	Receive correlation (u,l) for BS antenna n
$\mathbf{W}_u$	Weight matrix for phase beamforming
$\mathbf{V}_u$	Polarization matrix
$\mathbf{P}_u$	Power amplitude matrix
N	Number of dual-polarized antenna at BS
U	Number of users
α_{Lu},	Polarization leakage in LOS path
α_{Nu}	Polarization leakage in NLOS path
d_u,	Distance between BS and user u
ξ_u	Large scale fading coefficient
α_p, F_u	Path loss exponent, Shadow fading
Γ	Average channel gain at 1 m
ϖ	learning rate for WMMSE
γ_{th}^s,	Threshold SINR for ST
γ_{th}^t	Threshold SNR for TT
Superscript c	CSI available
Superscript l	Long-term channel statistics available
Superscript s & t	ST and TT respectively
Superscript r & i	Real and imaginary parts respectively
Subscript u	u^{th} user
Sets	$\mathscr{S}_1 = \{1, \cdots, U\}$, $\mathscr{S}_2 = \{1, \cdots, N\}$, $\mathscr{S}_3 = \{hh, hv, vh, vv\}$, $\mathscr{S}_4 = \{c, l\}$ $\mathscr{S}_5 = \{r, i\}$

and $\hat{\mathbf{X}}_u$ captures the polarization leakage given by

$$\hat{\mathbf{X}}_u = \begin{bmatrix} \sqrt{1-\alpha_{Nu}} & \sqrt{\alpha_{Nu}} \\ \sqrt{\alpha_{Nu}} & \sqrt{1-\alpha_{Nu}} \end{bmatrix}. \quad (7)$$

$\mathbf{G}_{un}$ has i.i.d. circularly symmetric complex Gaussian entries with entry $g^w_{un} \sim \mathscr{C}\mathscr{N}_c(0,1)$, $w \in \mathscr{S}_3$.

As multiple dual-polarized antennas are located at the base station, and multiple users are being served together by a single beam, spatial correlation in fading is also incorporated into the channel model. The spatial correlation may arise when scattering is not rich enough to decorrelate the elements of the channel matrix. The transmit correlation coefficient between m^{th} and n^{th} transmit antennas for user u is given by

$$\kappa^w_{mn,u} = \frac{\mathbb{E}[h^w_{un} h^{w*}_{um}]}{\sqrt{\mathbb{E}[|h^w_{um}|^2]}\sqrt{\mathbb{E}[|h^w_{un}|^2]}} = \frac{\mathbb{E}[h^w_{um} h^{w*}_{un}]}{\varphi_u}, m \neq n. \quad (8)$$

Similarly, the receiver correlation coefficient between u^{th} and l^{th} user for the n^{th} transmitter antenna is given by

$$\varrho^w_{ul,n} = \frac{\mathbb{E}[h^w_{un} h^{w*}_{ln}]}{\sqrt{\mathbb{E}[|h^w_{un}|^2]}\sqrt{\mathbb{E}[|h^w_{ln}|^2]}} = \frac{\mathbb{E}[h^w_{un} h^{w*}_{ln}]}{\varphi_u}, l \neq u. \quad (9)$$

where $w \in \mathscr{S}_3$. Here $\varphi_u = 1 - \alpha_{Nu}$ if $w \in \{hh, vv\}$, and $\varphi_u = \alpha_{Nu}$ otherwise. Since horizontal and vertical polarized antennas are colocated, they see the same scattering environment. Thus, equal statistical properties can be assumed across all four polarization channels, i.e., $\kappa^{hh}_{mn,u} = \kappa^{hv}_{mn,u} = \kappa^{vh}_{mn,u} = \kappa^{vv}_{mn,u}$ and $\varrho^{hh}_{ul,n} = \varrho^{hv}_{ul,n} = \varrho^{vh}_{ul,n} = \varrho^{vv}_{ul,n}$. Therefore, the NLOS channel can be expressed as

$$\hat{\mathbf{H}} = (\mathbf{1}_{U\times N} \otimes \hat{\mathbf{X}}) \odot (\mathbf{C}_r^{\frac{1}{2}} \mathbf{G} \mathbf{C}_t^{\frac{1}{2}}). \quad (10)$$

where $\mathbf{C}_t \in \mathbb{C}^{2N\times 2N}$ and $\mathbf{C}_r \in \mathbb{C}^{2U\times 2U}$ are the transmit and receive spatial correlation matrices respectively.

Remark 2. *It is notable from [24] that the cross polarization correlation is substantially less and its impact on systems sum spectral efficiency is negligible [25]. Thus, in this work we do not consider cross polarization correlation to keep the mathematical notation relatively simple.*

With the above channel model, we next formulate weighted sum rate optimization problem in multiaccess system using WMMSE algorithm for joint beamforming with long-term channel statistics as well as with CSI available at transmitter.

III. Performance Optimization in ST Scenario

In this section, we consider a scenario where all users are served simultaneously. Input symbol at each dual-polarized antenna is the weighted combination of elements of the symbol vector $\mathbf{s} = [s_1, s_2, \cdots, s_U]^T \in \mathbb{C}^{U\times 1}$ where s_u is the desired symbol of u^{th} user which is assumed to be independent with an average power of one, i.e., $\mathbb{E}[|\mathbf{s}_u|^2] = 1$. The signal observed at the user u is given by

$$y^s_u = \mathbf{q}^H_u \mathbf{H}_u \mathbf{W}_u \mathbf{T} s_u + \mathbf{q}^H_u \mathbf{H}_u \sum_{j=1, j\neq u}^{U} \mathbf{W}_j \mathbf{T} s_j + n_u \quad (11)$$

where $\mathbf{H}_u = [\mathbf{H}_{u1}, \mathbf{H}_{u2}, \cdots, \mathbf{H}_{uN}] \in \mathbb{C}^{2\times 2N}$ and $\mathbf{W}_u$ are the propagation channel and beamforming matrix of user u. $\mathbf{T} = [\mathbf{t}_1, \mathbf{t}_2, \cdots, \mathbf{t}_N]^T \in \mathbb{C}^{2N\times 1}$ is the transmit polarization vector. $\mathbf{W}_u$ is the block diagonal matrix whose n^{th} diagonal element corresponds to the complex weights for the n^{th}-u^{th} dual-polarized link. SINR for user u can be expressed as

$$\gamma^s_u = \frac{|\mathbf{q}^H_u \mathbf{H}_u \mathbf{W}_u \mathbf{T}|^2}{\sum_{j=1, j\neq u}^{U} |\mathbf{q}^H_u \mathbf{H}_u \mathbf{W}_j \mathbf{T}|^2 + \sigma_0^2}. \quad (12)$$

Thus, average weighted sum rate for ST is given by

$$R_{ST} = \mathbb{E}\left[\sum_{u=1}^{U} \beta_u \log_2(1 + \gamma^s_u)\right] \quad (13)$$

where $\beta_u > 0$ denotes the priority of u^{th} user to maintain fairness among the users. In the following subsections, we first define the beamforming terminology and then optimize the weighted sum rates for phase and joint beamforming.

We now present the beamforming possibilities with two aspects of EM waves, namely, *phase* and *polarization*.

1) Phase beamforming: In phase beamforming, the phase among multiple received signals are aligned at the desired location. In this case, the weight associated with each block matrix $\mathbf{W}_{un}$ becomes a complex scalar w_{un} for the n^{th} transmitter and u^{th} receiver pair; its amplitude is responsible for imparting power through phase synchronization. Therefore, for this scenario the weight matrix $\mathbf{W}_u$ can be written as

$$\mathbf{W}_u = \begin{bmatrix} w_{u1}[\mathbf{I}_2] & [\mathbf{0}] & \cdots & [\mathbf{0}] \\ [\mathbf{0}] & w_{u2}[\mathbf{I}_2] & \cdots & [\mathbf{0}] \\ . & . & \cdots & . \\ [\mathbf{0}] & [\mathbf{0}] & \cdots & w_{uN}[\mathbf{I}_2] \end{bmatrix} \in \mathbb{C}^{2N\times 2N}. \quad (14)$$

2) Joint beamforming: : It refers to both phase and polarization control for maximizing the SINR of the individual user. By phase control, our target is the same as discussed in the above subsection. By polarization control, we try to control the polarization of each received signal such that the desired signal components align constructively (maximum possible) with the receiver polarization and the undesired signal components align orthogonal (maximum possible) to the received signal. For joint beamforming, we split the weight matrix as

$$\mathbf{W}_u = \mathbf{P}_u \mathbf{V}_u \quad (15)$$

where $\mathbf{V}_u$ is a block diagonal polarization matrix given by

$$\mathbf{V}_u = \begin{bmatrix} [\mathbf{V}_{u1}] & [\mathbf{0}] & \cdots & [\mathbf{0}] \\ [\mathbf{0}] & [\mathbf{V}_{u2}] & \cdots & [\mathbf{0}] \\ . & . & \cdots & . \\ [\mathbf{0}] & [\mathbf{0}] & \cdots & [\mathbf{V}_{uN}] \end{bmatrix} \in \mathbb{C}^{2N\times 2N}. \quad (16)$$

The individual block matrix $\mathbf{V}_{un}$ is responsible for optimal phase and polarization design of the n^{th} transmitter antenna with respect to the u^{th} receiver. The power amplitude matrix $\mathbf{P}_u$ for user u can be written as

$$\mathbf{P}_u = \begin{bmatrix} \sqrt{p_{u1}}[\mathbf{I}_2] & [\mathbf{0}] & \cdots & [\mathbf{0}] \\ [\mathbf{0}] & \sqrt{p_{u2}}[\mathbf{I}_2] & \cdots & [\mathbf{0}] \\ . & . & \cdots & . \\ [\mathbf{0}] & [\mathbf{0}] & \cdots & \sqrt{p_{uN}}[\mathbf{I}_2] \end{bmatrix} \in \mathbb{C}^{2N\times 2N}. \quad (17)$$

Each entry of matrix $\mathbf{P}_u$ is real. The power allocated to the n^{th} dual-polarized antenna for the u^{th} user is p_{un}. From the weight matrices in (14), (16), and (17), we observe that polarization-aided beamforming increases the dimensionality of the system. We first formulate the optimization problem with phase beamforming and then present the joint beamforming case.

A. Sum Rate Maximization with Only Phase Beamforming

Weighted sum rate maximization for ST is formulated as

$$(\mathrm{P1}): \max_{\mathbf{W}} \quad R_{ST} \tag{18a}$$

$$\text{s.t.} \quad \sum_{u=1}^{U}\sum_{n=1}^{N}|w_{un}|^2 \leq P_t \tag{18b}$$

$$\mathbb{E}[\gamma_u^s] \geq \gamma_{th}^s \quad \forall u \in \mathscr{S}_1 \tag{18c}$$

where $\mathbf{W} = [\mathbf{W}_1, \mathbf{W}_2, \cdots, \mathbf{W}_U]$ and γ_u^s is the SINR. The objective in (18a) is non-convex with respect to $\mathbf{W}$. Constraint (18b) ensures that the total power of base station antennas does not exceed a given power budget P_t. The SINR guarantee constraint in (18c) is non-convex. It ensures that users being simultaneously served must have SINR above a threshold γ_{th}^s. Thus, P1 is non-convex. Next, we describe a methodology to convexify (18a) and (18c) and solve P1 considering CSI available and only long-term channel statistics at the transmitter.

1) Solution strategy with CSI available at transmitter: In this scenario, we consider that perfect CSI is available at the transmitter. Thus, the channel varies at block level and optimization is solved dedicatedly for each coherence block. First, we convexify the constraint in (18c). In the presence of CSI, $\mathbb{E}[\gamma_u^s] = \gamma_u^s$. If $\mathbf{W}_u\mathbf{T}$ is the solution then $\mathbf{W}_u\mathbf{T}e^{j\theta_u}$ is also another solution, for any $\theta_u \in \mathbb{R}$. Without loss of optimality, we exploit this phase ambiguity to rotate the phase such that the inner product $\mathbf{q}_u^H\mathbf{H}_u\mathbf{W}_u\mathbf{T}$ is real valued and positive. Therefore, condition $\gamma_u^s > \gamma_{th}^s$ can be rewritten as

$$\frac{1}{\sqrt{\gamma_{th}^s}}\Re\{\mathbf{q}_u^H\mathbf{H}_u\mathbf{W}_u\mathbf{T}\} \geq \sqrt{\sum_{\substack{j=1\\ j\neq u}}^{U}|\mathbf{q}_u^H\mathbf{H}_u\mathbf{W}_j\mathbf{T}|^2 + \sigma_0^2}. \tag{19}$$

The reformulated SINR constraint is the SOCP constraint, which is convex. To solve P1, we utilize the popular WMMSE algorithm to transform the objective in (18a) into convex form. The estimated data symbol at the receiver is $\hat{s}_u = a_u^c y_u^s$ where $a_u^c \in \mathbb{C}$ is the complex receiver gain with CSI for user u. Next, we compute mean square error (MSE) at the u^{th} user for the considered dual-polarized channel model given as

$$\begin{aligned} e_u^c = \mathbb{E}_{s_u}[||\hat{s}_u - s_u||^2] &= \sum_{j=1}^{U}|a_u^c|^2|(\mathbf{q}_u)^H\mathbf{H}_u\mathbf{W}_j\mathbf{T}|^2 + 1 \\ &- (a_u^c)^*(\mathbf{H}_u\mathbf{W}_u\mathbf{T})^H q_u - a_u^c(q_u)^H\mathbf{H}_u\mathbf{W}_u\mathbf{T} + |a_u^c|^2\sigma_0^2. \end{aligned} \tag{20}$$

Under the above modification the optimization problem (P1) under the WMMSE framework can be written as

$$(\mathrm{P2}): \min_{\mathbf{W},\mathbf{b}^c,\mathbf{a}^c} \quad \sum_{u=1}^{U}\beta_u^c(b_u^c e_u^c - \log_2 b_u^c) \quad \text{s.t. (18b) and (19).} \tag{21}$$

The problem (P2) is convex in each optimization variable $\mathbf{a}^c$, $\mathbf{b}^c$, and $\mathbf{W}$ individually, but not jointly. Therefore, a local optimum can be computed by iteratively optimizing over one variable while fixing the others. Using the first order optimality conditions, the MMSE receive filter and weight at user u for the considered dual-polarized system model respectively computed as

$$a_u^c = \arg\min_{a_u^c}\mathbb{E}[||\hat{s}_u - s_u||^2] = \frac{(\mathbf{q}_u)^H\mathbf{H}_u\mathbf{W}_u\mathbf{T}}{\sum_{j=1}^{U}|\mathbf{q}_u^H\mathbf{H}_u\mathbf{W}_j\mathbf{T}|^2+\sigma_0^2}, \tag{22}$$

$$b_u^c = \frac{\sum_{j=1}^{U}|\mathbf{q}_u^H\mathbf{H}_u\mathbf{W}_j\mathbf{T}|^2 + \sigma_0^2}{\sum_{\substack{j=1\\ j\neq u}}^{U}|\mathbf{q}_u^H\mathbf{H}_u\mathbf{W}_j\mathbf{T}|^2 + \sigma_0^2}, \tag{23}$$

where $u \in \mathscr{S}_1$, $\mathbf{a}^c = [a_1^c, a_2^c, \cdots, a_U^c]$, $\mathbf{b}^c = [b_1^c, b_2^c, \cdots, b_U^c]$.

2) Solution strategy with long-term channel statistics at transmitter: In high mobility scenarios, it is challenging for the base station to obtain CSI in every coherence interval. Thus, it relies only on long-term channel statistics to detect their dedicated signal from the received signal in (11). Solution strategy is similar to that in the previous case. However, as only channel statistics are available, while solving (P1) a few of the above equations are updated as follows:

It is notable that if $\gamma_u^s \geq \gamma_{th}$ for every channel instance, then (18c) is also satisfied. Thus, in order to convexify the constraint, we relax the average condition, which gives us the condition in (19). Now, in order to approximate the constraint (18c), we take expectation on both sides giving,

$$\mathbb{E}\left[\frac{1}{\sqrt{\gamma_{th}}}\Re\{\mathbf{q}_u^H\mathbf{H}_u\mathbf{W}_u\mathbf{T}\}\right] \geq \mathbb{E}\left[\sqrt{\sum_{\substack{j=1\\ j\neq u}}^{U}|\mathbf{q}_u^H\mathbf{H}_u\mathbf{W}_j\mathbf{T}|^2+\sigma_0^2}\right] \tag{24}$$

for all $u \in \mathscr{S}_1$. Tightness of the above constraint is verified in Section V. The MSE at the receiver under long-term channel statistics is computed as

$$\begin{aligned} e_u^l = \mathbb{E}_{s_u,\mathbf{H}_u}[||\hat{s}_u - s_u||^2] &= \sum_{j=1}^{U}|a_u|^2\mathbb{E}[|\mathbf{q}_u^H\mathbf{H}_u\mathbf{W}_j\mathbf{T}|^2]+1 \\ &- \mathbb{E}[(a_u^l)^*(\mathbf{H}_u\mathbf{W}_u\mathbf{T})^H q_u] - \mathbb{E}[a_u^l q_u^H\mathbf{H}_u\mathbf{W}_u\mathbf{T}] + |a_u^l|^2\sigma_0^2 \end{aligned} \tag{25}$$

where $a_u^l \in \mathbb{C}$ is the receiver gain with long-term channel statistics. P1 using WMMSE framework is revised as

$$(\mathrm{P3}): \min_{\mathbf{W},\mathbf{b}^l,\mathbf{a}^l} \quad \sum_{u=1}^{U}\beta_u^l(b_u^l e_u^l - \log_2 b_u^l) \quad \text{s.t. (18b) and (24).} \tag{26}$$

Similar to the previous case, (P3) is convex for each optimization variable individually but not jointly. With only long-term channel statistics, MMSE receive filter coefficient a_u^l and weight b_u^l, $u \in \mathscr{S}_1$ are computed as

$$a_u^l = \frac{\mathbb{E}[(\mathbf{q}_u)^H\mathbf{H}_u\mathbf{W}_u\mathbf{T}]}{\mathbb{E}\left[\sum_{j=1}^{U}|\mathbf{q}_u^H\mathbf{H}_u\mathbf{W}_j\mathbf{T}|^2\right] + \sigma_0^2}, \tag{27}$$

$$b_u^l = \frac{\mathbb{E}\left[\sum_{j=1}^{U} |\mathbf{q}_u^H \mathbf{H}_u \mathbf{W}_j \mathbf{T}|^2\right] + \sigma_0^2}{\mathbb{E}\left[\sum_{j=1}^{U} |\mathbf{q}_u^H \mathbf{H}_u \mathbf{W}_j \mathbf{T}|^2\right] + \sigma_0^2 - |\mathbb{E}[\mathbf{q}_u^H \mathbf{H}_u \mathbf{W}_u \mathbf{T}]|^2}. \quad (28)$$

From the above discussion, we conclude that optimization problem (P1) is reformulated to (P2) when CSI is available and to (P3) with only long-term channel statistics. In each iteration, we update the weight factor β_u at the t^{th} iteration in order to maintain fairness among the users as follows:

$$\beta_{\mathbf{u}}{}^{z,(t+1)} = \beta_{\mathbf{u}}{}^{z,(t)} + \varpi(\mathbf{R}^z - R_{avg}^z). \quad (29)$$

$z \in \mathscr{S}_4$, $\mathbf{R}^z = [R_1^z, R_2^z, \cdots, R_U^z]^T$ is the rate vector carrying rates allocated to each user. R_{avg} is the average rate of users.

Remark 3. *Phase beamforming can also be considered as the single polarization case as polarization is not optimized, and transmitter and receivers assume fixed polarization states.*

B. Sum Rate Maximization with Joint Beamforming

In this subsection, we formulate the optimization problem with joint beamforming at the receiver and propose a solution strategy for the same. Using (15), weighted sum rate maximization problem with joint beamforming is formulated as

$$\begin{aligned}
(\mathrm{P4}): \max_{\mathbf{V},\mathbf{P}} \quad & R_{ST} && (30a)\\
\text{s.t.} \quad & \sum_{u=1}^{U}\sum_{n=1}^{N} p_{un} \le P_t && (30b)\\
& \mathbf{V}_{un}^H \mathbf{V}_{un} = \mathbf{I}_2 \quad \forall\ n \in \mathscr{S}_2, u \in \mathscr{S}_1 && (30c)\\
& \text{and (18c)}
\end{aligned}$$

where $\mathbf{V} = [\mathbf{V}_1, \mathbf{V}_2, \cdots, \mathbf{V}_U]$ and $\mathbf{P} = [\mathbf{P}_1, \mathbf{P}_2, \cdots, \mathbf{P}_U]$. The objective in (30a) is non-convex with respect to $\mathbf{V}$ and $\mathbf{P}$. (30b) is the power budget constraint similar to (18b) reformulated in terms of the power matrix elements. Constraint (30c) ensure that the transmitter antenna polarization must not impart gain to the received signal. Constraints (30c) and (18c) are non-convex. Thus, (P4) is non-convex with respect to $\mathbf{V}$ and $\mathbf{P}$.

For mathematical tractability we first reduce the order of the constraints by defining $\mathbf{f}_{un} = \mathbf{V}_{un}\mathbf{t}_n = [f_{un}^h\ f_{un}^v]^T \in \mathbb{C}^{2\times 1}$. Also, $\mathbf{F} = [\mathbf{F}_1, \mathbf{F}_2, \cdots, \mathbf{F}_U]$ and $\mathbf{F}_u = [\mathbf{f}_{u1}, \mathbf{f}_{u2}, \cdots, \mathbf{f}_{uN}]^T \in \mathbb{C}^{2N\times 1}$. Thus, the constraint (18c) can be re-written as

$$\mathbf{f}_{un}^H \mathbf{f}_{un} = 1, \quad \forall\ u \in \mathscr{S}_1, n \in \mathscr{S}_2. \quad (31)$$

It is notable that the constraint in (31) is still non-convex. To convexify it, we rewrite it as

$$\mathbf{f}_{un}^H \mathbf{f}_{un} \le 1, \quad \forall\ u \in \mathscr{S}_1, n \in \mathscr{S}_2. \quad (32)$$

To meet the unit norm requirement of the polarization vectors, we normalize it after every iteration. To balance sum rate, we adjust normalization factor in the power allocated to each user. We note that problem (P4) is similar to problem (P1) with additional polarization constraint. Thus, we again propose the use of WMMSE framework to solve the above optimization.

1) Solution strategy with CSI available at transmitter: In the presence of CSI, $\mathbb{E}[\gamma_u^s] = \gamma_u^s$. Following the similar argument as for phase beamforming we can say that $\mathbf{P}_u\mathbf{F}_u$ and $\mathbf{P}_u\mathbf{F}_u e^{j\theta_u}$ are equivalent. Therefore, the condition $\gamma_u^s > \gamma_{th}^s$ can be formulated as SOCP constraint as

$$\frac{1}{\sqrt{\gamma_{th}^s}} \Re\{\mathbf{q}_u^H \mathbf{H}_u \mathbf{P}_u \mathbf{F}_u\} \ge \sqrt{\sum_{\substack{j=1 \\ j\neq u}}^{U} |\mathbf{q}_u^H \mathbf{H}_u \mathbf{P}_j \mathbf{F}_j|^2 + \sigma_0^2}. \quad (33)$$

Under the above-mentioned modifications, the optimization problem (P4) under WMMSE framework can be written as

$$\begin{aligned}
(\mathrm{P5}): \min_{\mathbf{F},\mathbf{P},\mathbf{b}^c,\mathbf{a}^c} \quad & \sum_{u=1}^{U} \beta_u^c (b_u^c e_u^c - \log_2 b_u^c) && (34)\\
\text{s.t.} \quad & (30\text{b}), (32), (33)
\end{aligned}$$

where e_u^c, b_u^c, and a_u^c are given in (20), (22) and (23) with $\mathbf{W}_u\mathbf{T}$ replaced with $\mathbf{P}_u\mathbf{F}_u$. To obtain optimal values of $\mathbf{P}$ and $\mathbf{F}$, we divide the optimization problem into two subproblems and solve them alternately using WMMSE framework. The two sub-problems can be stated as

$$\begin{aligned}
(\mathrm{P51}): \min_{\mathbf{F}} \quad & \sum_{u=1}^{U} \beta_u^c (b_u^c e_u^c - \log_2 b_u^c) && (35)\\
\text{s.t.} \quad & (32) \text{ and } (33),
\end{aligned}$$

$$\begin{aligned}
(\mathrm{P52}): \min_{\mathbf{P}} \quad & \sum_{u=1}^{U} \beta_u^c (b_u^c e_u^c - \log_2 b_u^c) && (36)\\
\text{s.t.} \quad & (30\text{b}) \text{ and } (33).
\end{aligned}$$

2) Solution strategy with long-term channel statistics at transmitter: Following the similar strategy as in Section III-A-2, the SOCP constraint can be approximated as

$$\mathbb{E}\left[\frac{1}{\sqrt{\gamma_{th}^s}} \Re\{\mathbf{q}_u^H \mathbf{H}_u \mathbf{P}_u \mathbf{F}_u\}\right] \ge \mathbb{E}\left[\sqrt{\sum_{\substack{j=1 \\ j\neq u}}^{U} |\mathbf{q}_u^H \mathbf{H}_u \mathbf{P}_j \mathbf{F}_j|^2 + \sigma_0^2}\right] \quad (37)$$

for $u \in \mathscr{S}_1$. Thus, (P4) is revised for ST with joint beamforming considering only long-term channel statistics as

$$\begin{aligned}
(\mathrm{P6}): \min_{\mathbf{F},\mathbf{P},\mathbf{b}^l,\mathbf{a}^l} \quad & \sum_{u=1}^{U} \beta_u^l (b_u^l e_u^l - \log_2 b_u^l) && (38)\\
\text{s.t.} \quad & (30\text{b}), (32), (37)
\end{aligned}$$

where e_u^l, a_u^l, and b_u^l are given in (25), (27), and (28) with $\mathbf{W}_u\mathbf{T}$ are replaced with $\mathbf{P}_u\mathbf{F}_u$. The optimization problem (P6) is also solved using alternating optimization. The two subproblems to obtain optimum $\mathbf{P}$ and $\mathbf{F}$ can be stated as

$$\begin{aligned}
(\mathrm{P61}): \min_{\mathbf{F}} \quad & \sum_{u=1}^{U} \beta_u^l (b_u^l e_u^l - \log_2 b_u^l) && (39)\\
\text{s.t.} \quad & (32) \text{ and } (37),
\end{aligned}$$

$$\begin{aligned}
(\mathrm{P62}): \min_{\mathbf{P}} \quad & \sum_{u=1}^{U} \beta_u^l (b_u^l e_u^l - \log_2 b_u^l) && (40)\\
\text{s.t.} \quad & (30\text{b}) \text{ and } (37).
\end{aligned}$$

For fairness, the weight factor β_u^z is updated as in (29).

Using the WMMSE framework, the weighted sum rate is

given by $\sum_{u=1}^{U} \beta_u \log_2 b_u^z, z \in \mathscr{S}_4$. Closed-form expression for the average rate with CSI at the transmitter is difficult to obtain as it makes optimal power, phase, and polarization functions of the instantaneous channel state. Since functional forms of these optimal parameters are not available, the closed forms for the expectations in (22) cannot be obtained and the average rate is computed by maximizing rate for every channel instantiation using the WMMSE structure. With only long-term channel statistics at the transmitter, optimal power, phase and polarization are function of channel statistical parameters, the expectations in (28) can be evaluated using Lemma 1.

Lemma 1. *The term* $\mathbb{E}\left[\sum_{j=1}^{U} |\boldsymbol{q}_u^H \boldsymbol{H}_u \boldsymbol{P}_j \boldsymbol{F}_j|^2\right]$ *can be simplified to obtain* $\mathbb{E}[\boldsymbol{\zeta}_{ju}^T \boldsymbol{\zeta}_{ju}]$, *where* $\boldsymbol{\zeta}_{ju} = [\zeta_{ju}^r, \zeta_{ju}^i]^T$ *follows bivariate Gaussian distribution with mean* $\boldsymbol{\mu}_{\zeta_{ju}} = \begin{bmatrix} \mu_{\zeta_{ju}^r}, & \mu_{\zeta_{ju}^i} \end{bmatrix}^T$ *and covariance matrix* $\mathbf{C}_{\zeta_{ju}} = \mathbb{E}[(\boldsymbol{\zeta}_{ju} - \boldsymbol{\mu}_{ju})(\boldsymbol{\zeta}_{ju} - \boldsymbol{\mu}_{ju})^T]$, *where* $\mu_{\zeta_{ju}^r}$, $\mu_{\zeta_{ju}^i}$, *and* $\sigma^2_{\zeta_{ju}}$ *are defined in* (41), (42) *and* (43), *respectively.*

Proof. See Appendix A. □

Substituting the result from Lemma 1 in b_u^l we obtain

$$b_u^l = \frac{\sum_{j=1}^{U} \mathbb{E}[\boldsymbol{\zeta}_{ju}^T \boldsymbol{\zeta}_{ju}] + \sigma_0^2}{\sum_{j=1}^{U} \mathbb{E}[\boldsymbol{\zeta}_{ju}^T \boldsymbol{\zeta}_{ju}] + \sigma_0^2 - |\mathbb{E}[\mathbf{q}_u^H \mathbf{H}_u \mathbf{P}_u \mathbf{F}]|^2}. \tag{44}$$

The average weighted sum rate in terms of channel statistical parameters derived in Lemma 1 is obtained in Lemma 2.

Remark 4. *By virtue of channel spatial correlation,* ζ_{ju}^r *and* ζ_{ju}^i *are correlated random variables.*

Remark 5. *The average weighted sum rate for only phase beamforming is again governed by Lemma 2 as the optimal phase is captured by* η_{jun}^w, $w \in \mathscr{S}_3$. *Therefore, the type of beamforming only impacts the value of* η_{jun}^w.

With CSI available, the detailed algorithmic procedure for solving the optimization for phase and joint beamforming is given in Algorithm 1, except that for phase beamforming steps 4 to 6 are excluded. With only long-term channel statistics available at the transmitter, phase and joint beamforming are governed by the Algorithm 2 except that the steps from 3 to 5 are excluded for phase beamforming. Furthermore, for phase beamforming, **P** is replaced with **W** and **F** is replaced with **T** and an initialized value of **T** is used throughout the algorithm. Both Algorithm 1 and 2 contains NK and $3NK$ variables for phase and joint beamforming, respectively. With CSI available at the transmitter, total computational complexity for phase beamforming simulated using WMMSE-based algorithm is $\mathbf{O}(SI_P(U^2N^2 + U^2N + UN))$ where I_P denotes the iteration count and S denotes the number of channel realizations. For joint beamforming total complexity is given by $\mathbf{O}(BSI_J(U^2N^2 + U^2N + 2UN))$ where B is the number of blocks in alternating optimization and I_J is the number of iterations for joint beamforming. For long-term channel statistics, the computational complexity is same as that of Algorithm 1 with $S = 1$. This is because algorithms with CSI available are computed on a small-scale fading, whereas algorithms with long-term channel statistics are computed on a large-scale fading. Thus, the total computational complexity of Algorithm 2 is much lower than that of Algorithm 1 [40].

Algorithm 1 Alternating optimization for ST with CSI

Input: N, U, $\mathbf{H}$, $\mathbf{q}_u$, P_n, ϖ
Initialize: $\mathbf{F}_{init}$, $\mathbf{P}_{init}$, β_{init}, $\mathbf{f}_u$

1: **for** channel instance=1: Total channel instances **do**
2: **for** iteration count=1 :Maximum iterations **do**
3: Compute a_u^c an b_u^c using (22) and (23) for all u
4: Compute e_u^c using (20) for all u and optimize $P51$ in (35) using CVX to obtain optimal $\mathbf{F}^*$.
5: Normalize $\mathbf{F}^*$ to satisfy constraint (32).
6: Adjusting magnitude: Update $\mathbf{P} \leftarrow \mathbf{P}||\mathbf{f}_{un}||_2 \forall\ u, n$.
7: Compute e_u^c using (25) for all u and optimize $P52$ in (36) using CVX to obtain optimal $\mathbf{P}^*$.
8: Compute $R_u = \log_2(b_u)$
9: Compute $R_{avg} = \sum_{u=1}^{U} R_u/U$
10: Update weight factor β_u using (29)
11: Normalize β_u such that $\sum_{u=1}^{U} \beta_u = 1$
12: Weighted sum rate $= \sum_{u=1}^{U} \beta_u R_u$
13: Check for stopping criterion: if met then break the loop, else continue.
14: **end for**
15: Compute R_{ST} corresponding to channel instances
16: **end for**

Output: $\mathbf{P}^*$, $\mathbf{F}^*$, β^*

Algorithm 2 Alternating optimization for ST with long-term channel statistics

Input: N, U, $\mathbf{H}$, $\mathbf{q}_u$, P_n, ϖ
Initialize: $\mathbf{F}_{init}$, $\mathbf{P}_{init}$, β_{init}, $\mathbf{f}_u$

1: **for** iteration count=1:Maximum number of iterations **do**
2: Compute a_u^l and b_u^l using (27) and (28) for all u
3: Compute e_u^l using (25) for all u and optimize $P61$ in (39) using CVX to obtain optimal $\mathbf{F}^*$.
4: Normalize $\mathbf{F}^*$ to satisfy constraint (32)
5: Adjusting magnitude: Update $\mathbf{P} \leftarrow \mathbf{P}||\mathbf{f}_{un}||_2 \forall\ u, n$.
6: Compute e_u^l using (25) for all u and optimize $P62$ in (40) using CVX to obtain optimal $\mathbf{P}^*$.
7: Follow the steps from (8) to (13) from Algorithm 1
8: **end for**

Output: $\mathbf{P}^*$, $\mathbf{F}^*$, β^*

IV. Performance Optimization in TT Scenario

We now consider a scenario where all users are served in a time-shared mode. In this scheme, a block of time duration is divided into U slots. The input symbol at each dual antenna to serve u^{th} user is $\mathbf{s} = s_u$. The fraction of total time allocated to u^{th} user is τ_u such that $\sum_{u=1}^{U} \tau_u = 1$. Thus, the signal received at user u in slot τ_u is $y_u^t = \mathbf{q}_u^H \mathbf{H}_u \mathbf{W}_u \mathbf{T} s_u + n_u$. The corresponding SNR is given by

$$\gamma_u^t = |\mathbf{q}_u^H \mathbf{H}_u \mathbf{W}_u \mathbf{T}|^2 / \sigma_0^2. \tag{45}$$

Data rate of user u is $\tau_u \log_2(1 + \gamma_u^t)$. Thus, the average weighted sum rate of the system under TT scenario is

$$R_{TT} = \mathbb{E}\left[\sum_{u=1}^{U} \beta_u \tau_u \log_2(1 + \gamma_u^t)\right]. \tag{46}$$

To maximize the sum rate in (46) under the total power, time, polarization norm, and SINR constraints of each user, optimization problem is formulated next.

Lemma 2. *The average weighted sum rate under simultaneous transmission is given by*

$$\sum_{u=1}^{U}\beta_u^l\log_2\left[\frac{\sum_{j=1}^{U}(2\sigma_{\zeta_{ju}}^2+\mu_{\zeta_{ju}}^{r2}+\mu_{\zeta_{ju}}^{i2})+\sigma_0^2}{\sum_{j=1}^{U}(2\sigma_{\zeta_{ju}}^2+\mu_{\zeta_{ju}}^{r2}+\mu_{\zeta_{ju}}^{i2})+\sigma_0^2-\xi_u^2\frac{K}{1+K}\left\{\left(\sum_{n=1}^{N}\left[(\eta_{jun}^{hhr}+\eta_{jun}^{vvr})\sqrt{1-\alpha_L}+(\eta_{jun}^{hvr}+\eta_{jun}^{vhr})\sqrt{\alpha_L}\right]\right)^2\right.}\right.$$
$$\left.\left.+\left(\sum_{n=1}^{N}\left[(\eta_{jun}^{hhi}+\eta_{jun}^{vvi})\sqrt{1-\alpha_L}+(\eta_{jun}^{hvi}+\eta_{jun}^{vhi})\sqrt{\alpha_L}\right]\right)^2\right\}\right]$$

Proof. See Appendix B. □

$$\mu_{\zeta_{1ju}}=\sqrt{\frac{K}{1+K}}\xi_u\sum_{n=1}^{N}\{\sqrt{1-\alpha_{Lu}}(\eta_{jun}^{hhr}+\eta_{jun}^{vvr})+\sqrt{\alpha_{Lu}}(\eta_{jun}^{hvr}+\eta_{jun}^{vhr})\}. \tag{41}$$

$$\mu_{\zeta_{2ju}}=\sqrt{\frac{K}{1+K}}\xi_u\sum_{n=1}^{N}\{\sqrt{1-\alpha_{Lu}}(\eta_{jun}^{hhi}+\eta_{jun}^{vvi})+\sqrt{\alpha_{Lu}}(\eta_{jun}^{hvi}+\eta_{jun}^{vhi})\}. \tag{42}$$

$$\begin{aligned}\sigma_{\zeta_{ju}}^2=\frac{\xi_u^2}{2}\left(\frac{1}{1+K}\right)\sum_{n=1}^{N}\sum_{m=1}^{N}\sum_{p=1}^{U}\sum_{q=1}^{N}\Big((\alpha_{Nu})\Big[&(\eta_{jun}^{vhi}\eta_{jum}^{hvi}+\eta_{jun}^{vhr}\eta_{jum}^{hvr})\delta_{up}^{t}\rho_{qmn}^{c}+(\eta_{jun}^{vhi}\eta_{jum}^{vhi}+\eta_{jun}^{vhr}\eta_{jum}^{vhr})\delta_{up}^{v}\rho_{qmn}^{b}\\&+(\eta_{jun}^{hvi}\eta_{jum}^{hvi}+\eta_{jun}^{hvr}\eta_{jum}^{hvr})\delta_{up}^{h}\rho_{qmn}^{a}+(\eta_{jun}^{hvi}\eta_{jum}^{vhi}+\eta_{jun}^{hvr}\eta_{jum}^{vhr})\delta_{up}^{t}\rho_{qmn}^{d}\Big]+(1-\alpha_{Nu})\Big[(\eta_{jun}^{vvi}\eta_{jum}^{hhi}+\eta_{jun}^{vvr}\eta_{jum}^{hhr})\delta_{up}^{t}\rho_{qmn}^{d}\\&+(\eta_{jun}^{vvi}\eta_{jum}^{vvi}+\eta_{jun}^{vvr}\eta_{jum}^{vvr})\delta_{up}^{v}\rho_{qmn}^{a}+(\eta_{jun}^{hhi}\eta_{jum}^{hhi}+\eta_{jun}^{hhr}\eta_{jum}^{hhr})\delta_{up}^{h}\rho_{qmn}^{b}+(\eta_{jun}^{hhi}\eta_{jum}^{vvi}+\eta_{jun}^{hhr}\eta_{jum}^{vvr})\delta_{up}^{t}\rho_{qmn}^{c}\Big]\\&+\sqrt{(1-\alpha_{Nu})(\alpha_{Nu})}\Big[(\eta_{jun}^{vhi}\eta_{jum}^{vvi}+\eta_{jun}^{vhr}\eta_{jum}^{vvr})\delta_{up}^{v}\rho_{qmn}^{3}+(\eta_{jun}^{vvi}\eta_{jum}^{vhi}+\eta_{jun}^{vvr}\eta_{jum}^{vhr})\delta_{up}^{v}\rho_{qmn}^{d}+(\eta_{jun}^{hvi}\eta_{jum}^{vvi}+\eta_{jun}^{hvr}\eta_{jum}^{vvr}\\&+\eta_{jun}^{vvi}\eta_{jum}^{hvi}+\eta_{jun}^{vvr}\eta_{jum}^{hvr})\delta_{up}^{t}\rho_{qmn}^{a}+(\eta_{jun}^{vhi}\eta_{jum}^{hhi}+\eta_{jun}^{vhr}\eta_{jum}^{hhr}+\eta_{jun}^{hhi}\eta_{jum}^{vhi}+\eta_{jun}^{hhr}\eta_{jum}^{vhr})\delta_{up}^{t}\rho_{qmn}^{b}\\&+(\eta_{jun}^{hhi}\eta_{jum}^{hvi}+\eta_{jun}^{hhr}\eta_{jum}^{hvr})\delta_{up}^{h}\rho_{qmn}^{c}+(\eta_{jun}^{hvi}\eta_{jum}^{hhi}+\eta_{jun}^{hvr}\eta_{jum}^{hhr})\delta_{up}^{h}\rho_{qmn}^{d}\Big]\Big).\end{aligned} \tag{43}$$

A. Sum Rate Maximization with Phase Beamforming

For phase beamforming, the average weighted sum rate can be obtained using (46) by substituting (45). The weighted sum rate maximization problem is formulated as

$$(\text{P7}):\max_{\tau,\mathbf{P}}\quad R_{TT} \tag{47a}$$
$$\sum_{n=1}^{N}p_{un}\le P_t\ \ \forall u\in\mathscr{S}_1 \tag{47b}$$
$$\tau_u\mathbb{E}[\gamma_u^t]\ge\gamma_{th}^t\ \ \forall u\in\mathscr{S}_1 \tag{47c}$$
$$\sum_{u=1}^{U}\tau_u=1. \tag{47d}$$

In TT as each user is served individually, phases of base station antennas are adjusted to equalize the impact of channel and match with the receiver polarization. The optimal phase depends on CSI availability at the transmitter and is given by

$$\phi_{un}^c=\angle\mathbf{q}^H\mathbf{H}_{nu}\mathbf{t}_{nu};\text{with CSI}, \tag{48}$$

$$\phi_{un}^l=\angle\mathbf{q}^H\mathbb{E}[\mathbf{H}_{nu}]\mathbf{t}_{nu};\text{with long-term statistics}. \tag{49}$$

As the total available power is allocated to each user, P_t is divided among all transmit antennas. The fraction of time for which each user is served depends on the transmitter-receiver channel conditions, i.e., if the channel is good, less fraction of time is allocated in order to satisfy constraint (47c). Each time slot τ_u is selected such that the constraint (47d) is satisfied.

B. Sum Rate Maximization with Joint Beamforming

For joint beamforming, the average weighted sum rate is obtained using (46) by substituting (15) and (45). Here, the optimization problem remains the same as in (P7) with additional constraint (30c). Similar to ST, we rewrite polarization norm constraint (30c) as (31). Thus, optimization variable $\mathbf{V}$ is replaced with $\mathbf{F}$ in (P7) and the SNR in (45) is updated to

$$\gamma_u^t=|\mathbf{q}_u^H\mathbf{H}_u\mathbf{P}_u\mathbf{F}_u|^2/\sigma_0^2. \tag{50}$$

We first adjust the polarization of each transmit antenna such that it nullifies the channel and matches with the receiver polarization. The optimal polarization vectors are given by

$$\mathbf{f}_{un}^c=\frac{(\mathbf{g}_u^H\mathbf{H}_{un})^H}{||\mathbf{g}_u^H\mathbf{H}_{un}||_2};\ \text{with CSI}, \tag{51a}$$

$$\mathbf{f}_{un}^l=\frac{(\mathbf{g}_u^H\mathbb{E}[\mathbf{H}_{un}])^H}{||\mathbf{g}_u^H\mathbb{E}[\mathbf{H}_{un}]||_2};\ \text{with long-term statistics}. \tag{51b}$$

Note that division by norm values in (51a) and (51b) ensure that constraint (31) is satisfied. Optimal phase is given as

$$\phi_{un}^c=\angle\mathbf{q}^H\mathbf{H}_{nu}\mathbf{f}_{nu}^c;\ \text{with CSI}, \tag{52a}$$

$$\phi_{un}^l=\angle\mathbf{q}^H\mathbb{E}[\mathbf{H}_{nu}]\mathbf{f}_{nu}^l;\ \text{with long-term statistics}. \tag{52b}$$

In TT, the weight factor β_u is iteratively updated as in ST using (29). Similar to ST, with CSI available at the transmitter, closed form for the average weighted sum rate cannot be obtained as optimal parameters are the functions of channel state. However, with long-term channel statistics, expectations can be evaluated. Using Jensen's inequality, the upper bound for average weighted sum rate in (46) can be obtained as

$$R_{TT}\le\sum_{u=1}^{U}\beta_u\tau_u\log_2(1+\mathbb{E}[\gamma_u^t]). \tag{53}$$

Using Lemma (1) we obtain

$$\mathbb{E}[|\mathbf{q}_u^H\mathbf{H}_u\mathbf{P}_u\mathbf{F}_u|^2]=\mathbb{E}[\boldsymbol{\zeta}_{uu}^T\boldsymbol{\zeta}_{uu}], \tag{54}$$

where $\boldsymbol{\zeta}_{uu}=[\zeta_{uu}^r,\zeta_{uu}^i]$. ζ_{uu}^r, and ζ_{uu}^i can be obtained using the (A.4) and (A.5) which are still Gaussian distributed with

mean and variance governed by (41), (42) and (43). Using (54), average SNR in TT is $\mathbb{E}[\gamma_u^t] = \frac{\mathbb{E}[\boldsymbol{\zeta}_{uu}^T \boldsymbol{\zeta}_{uu}]}{\sigma_0^2}$. To compute $\mathbb{E}[\boldsymbol{\zeta}_{uu}^T \boldsymbol{\zeta}_{uu}]$ we use the moment generating function approach similar to that in Appendix B and obtain

$$\mathbb{E}[\gamma_u^t] = (2\sigma_{uu}^2 + (\mu_{uu}^r)^2 + (\mu_{uu}^i)^2)/\sigma_0^2. \tag{55}$$

Substituting the above computed value in (50), the average weighted sum rate in TT is upper bounded by

$$R_{TT} \leq \sum_{u=1}^{U} \beta_u \tau_u \log_2 \left(1 + \frac{2\sigma_{uu}^2 + (\mu_{uu}^r)^2 + (\mu_{uu}^i)^2)}{\sigma_0^2}\right). \tag{56}$$

With CSI available, the detailed algorithmic procedure for sum rate maximization in TT for phase and joint beamforming is given in Algorithm 3, except that for phase beamforming step 3 is relaxed and the step 4 of optimal phase determination is governed by (48). Similarly, when only long-term channel statistics are available, Algorithm 4 is used to obtain the solution except that step 2 is relaxed and step 3 is governed by (49). Additionally, for phase beamforming, $\mathbf{P}$ and $\mathbf{F}$ are replaced with $\mathbf{W}$ and $\mathbf{T}$ and an initialized value of $\mathbf{T}$ is used. Both Algorithm 3 and 4 contains NK and $3NK$ variables for phase and joint beamforming respectively. Computational complexity of phase and joint beamforming with CSI available at the transmitter is $\mathbf{O}(SU(N^2+N))$ and $\mathbf{O}(SU(N^2+2N))$, respectively. Following the similar argument as given for ST in Section III, computational complexity for long-term channel statistics is same as that with CSI available with $S = 1$.

Algorithm 3 Beamforming Algorithm for TT with CSI

Input: N, U, $\mathbf{H}$, $\mathbf{q}_u$, P_n, ϖ
Initialize: β_{init}, $\mathbf{f}_u$
Output: $\mathbf{P}^*$, $\mathbf{F}^*$, β^*, τ^*

1: **for** channel instance=1:Total channel instances **do**
2: Compute $\mathbf{f}_{un}^c$ using (51a)
3: Compute ϕ_{un}^l using (52a)
4: Set $p_{un} = \frac{P_t}{N}$
5: Compute $\tau_u = \frac{\gamma_t}{\gamma_u}$.
6: **if** $\sum_{u=1}^{U} \tau_u > 1$ **then**
7: Select users with higher rates satisfying (47c)
8: **else**
9: Scale each τ_u by equally to satisfy (47c)
10: **end if**
11: Compute $R_u = \tau_u \log_2(1+\gamma_u)$
12: Compute $R_{avg} = \sum_{u=1}^{U} R_u/U$
13: Update weight factor β_u using (29)
14: Normalize β_u such that $\sum_{u=1}^{U} \beta_u = 1$
15: Check for stopping criterion: if met, then break the loop, else continue.
16: **end for**

Algorithm 4 Beamforming Algorithm for TT with long-term channel statistics

Input: N, U, $\mathbf{H}$, $\mathbf{q}_u$, P_n, ϖ
Initialize: β_{init}, $\mathbf{f}_u$
Output: $\mathbf{P}^*$, $\mathbf{F}^*$, β^*, τ^*

1: Compute $\mathbf{f}_{un}^l$ using (51b)
2: Compute ϕ_{un}^l using (52b)
3: Follow the steps from (4) to (16) from Algorithm 3.

V. Results and Discussion

In this section, we evaluate the performance of a single cell multi-user system. We analyze users that are independently and uniformly distributed within a sector of radius of 500 m. The base station is located at the center and is assumed to be elevated at 20 m. The large-scale fading coefficient in dB is modeled as $\xi_u = \Gamma - 10\alpha_p \log_{10}(d_u/1\text{m}) + F_u$ [25] where $F_u \sim \mathcal{N}(0, \sigma_{sf}^2)$ with $\sigma_{sf} = 7$, $\alpha_p = 3.76$ and $\Gamma = -35.3$. LOS and NLOS channel XPDs are considered to be 15 dB and 5 dB, respectively for all users [23]. $\kappa_{mn,u}^w = 0$, $\varrho_{mn,u}^w = 0$, $w \in \mathscr{S}_3$, and $\varpi = 10^{-5}$. Initial weight vector $\beta_{init} = \mathbf{1}_{1\times U}$, $\forall u \in U$. We consider $\gamma_{th}^s = \gamma_{th}^t = \gamma_{th}$. For simulation any initial value for power amplitude matrix and polarization vector can be taken. In the following subsections, we compare the average weighted sum rate performance of ST with TT under both joint beamforming and only phase beamforming. We also study the impact of various system and channel parameters and CSI on them. To capture different system and channel aspects, simulation is carried out for different parameters, which are stated at the beginning of each subsection. Simulations are conducted in MATLAB using CVX (SDPT3 solver) [41] on a standard desktop machine with Intel(R) Core(TM) i9-10900 CPU @ 2.80 GHz processor.

A. Performance of Polarization-Integrated WMMSE

1) Convergence performance of beamforming strategies: Fig. 2(a) shows the performance of polarization-integrated WMMSE algorithm in computing average weighted sum rate and selecting optimal power values. Simulation is performed for $U = 4$, $N = 10$, $\gamma_{th} = -15$ dB, $P_t = 10$ dBm and $K = 0$ dB. Iteration counts are provided to show that the sum rate converges in approximately 10 iterations for both the cases. Additionally, higher weighted sum rate is obtained for joint beamforming compared to only phase beamforming. This is due to the polarization beamforming of user with the desired signal and nullforming with the undesired signal.

2) Optimality of WMMSE: To maximize the weighted sum rate for ST, we have proposed WMMSE-based solutions in polarization domain which is a locally convergent approach. We benchmark its performance against the globally optimal solution using the branch-and-bound (BNB) method [37], [42]. Owing to its high computational complexity, BNB is applied to small-scale scenarios and serves as the performance upper bound for evaluating the proposed WMMSE-based methods. Fig. 2(b) compares the performance of WMMSE against BNB. Simulation parameters: $N = 6$, $U = 2$, $K = -10$ dB, and $\gamma_{th} = -15$ dB. We observe that BNB being a globally convergent approach gave better rates in comparison to WMMSE. However, these gains were obtained at the cost of time. For example, for joint beamforming with transmit power of 20 dBm, additional gain of $\approx 1.5\%$ was obtained with BNB at the cost of ≈ 60 times extra time with respect to WMMSE.

For large-scale scenarios, we validate the optimality using duality gap. Fig. 2(c) validates the optimality of WMMSE algorithm in solving optimization with CSI available. Simulation paramters: $U = 4$, $N = 10$, $\gamma_{th} = -15$ dB, $P_t = 10$ dBm and $K = 0$ dB. Optimization algorithms show duality gap on

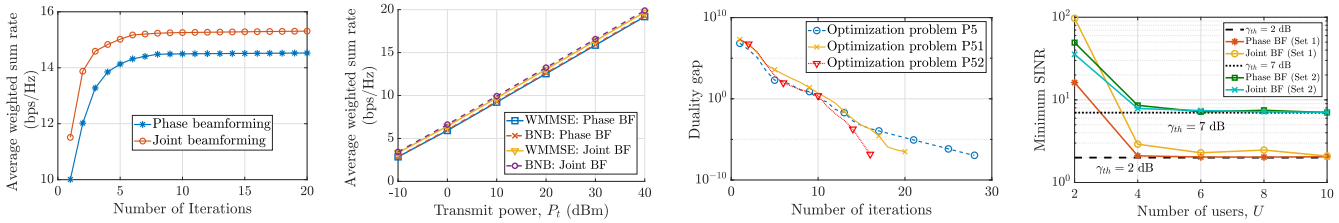

(a) (b) (c) (d)

Fig. 2: (a) Polarization integrated WMMSE performance, (b) Performance benchmarking with BNB, (c) Validation of WMMSE algorithm, (d) Verification of SOCP approximation in (24) and (37). Set 1: P_t=15 dBm, γ_{th}=2 dB, Set 2: P_t=25 dBm, γ_{th}=7 dB, BF: beamforming.

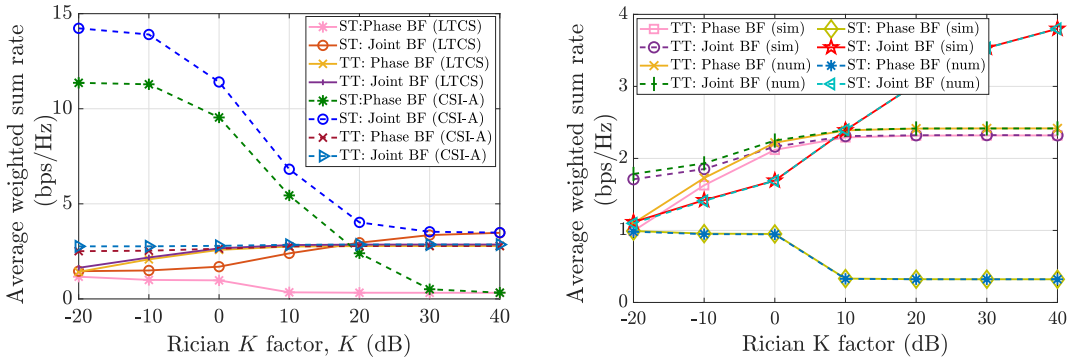

(a) (b)

Fig. 3: (a) Performance comparison of joint beamforming with phase beamforming under ST and TT, (b) Verification for weighted sum rate performance. sim: simulation, num: numerical, BF: beamforming, CSI-A: CSI available, LTCS: long-term channel statistics.

the orders of 10^{-7} (typical acceptable values are on the order of 10^{-5} [43]) in 15, 27, and 19 iterations for P5, P51 and P52, respectively, thereby leading the solution for phase and joint beamforming close to the true optimal. Thus, WMMSE is suitable for resource allocation in the proposed framework as it gives near-optimal performance. Additionally, WMMSE is practical for large-scale systems due to its polynomial time complexity. Also, the closed-form updates in WMMSE makes the implementation easy and fast.

3) Tightness of SOCP constraint: In Section III, the SOCP constraint under long-term channel statistics is approximated as (24) and (37) for phase and polarization beamforming respectively. Fig. 2(d) verifies the tightness of the approximation by plotting the minimum SINR values assigned to each user with respect to U. The constraint is verified for two sets of transmit power and threshold SINR values for both phase and joint beamforming. $N = 10$, $K = 5$ dB is considered. We observed that as U increases, minimum SINR value allocated by the approximate SOCP constraint to the user decreases. However, it does not fall below the threshold SINR.

B. Impact of K on Beamforming Strategies in Multiaccess

In this subsection, we compare the performance of joint beamforming with phase beamforming, ST with TT, and study the impact of CSI for different channel conditions captured by the Rician K-factor as shown in Fig. 3(a). For this performance comparison study, simulation is performed for $U = 5$, $N = 6$, $\gamma_{th} = -20$ dB and $P_t = 20$ dB.

1) Performance comparison of joint beamforming and phase beamforming: Fig. 3(a) shows that joint beamforming performs better than only phase beamforming, with average performance improvement of 23% and 5.53% with CSI and 89.19% and 4.2% with long-term channel statistics for ST and TT, respectively. These additional gains are obtained by virtue of signal enhancement at the intended user via polarization beamforming and interference mitigation at the unintended user antenna via polarization orthogonality.

Furthermore, ST with joint and phase beamforming exhibit opposite trends, i.e., the former increases and the latter decreases with K factor with long-term channel statistics. At low K values, channel diversity provided by the multipath dominant channel allows at least one user to be served with higher SINR guarantee and the rest are served close to the SINR threshold for both phase and joint beamforming. At high K factor, due to statistically identical paths, interference is not sufficiently canceled for all the users, thereby serving them fairly close to SINR threshold for phase beamforming. However, with joint beamforming polarization orthogonality allows at least two users to be served with higher SINR guarantee and serving the rest close to SINR threshold. In TT as there is no interference term, average weighted sum rate follows the same trend for phase and joint beamforming.

Remark 6. *At high K values, with long-term channel statistics at the transmitter, polarization beamforming in addition to phase beamforming is necessary for ST to outperform TT.*

2) Performance comparison of ST and TT: From Fig. 3(a), we also observe that at low K factors with CSI available, ST outperforms TT due to sufficient interference cancellation by virtue of channel diversity thereby making γ_u^s and γ_u^t equivalent. In TT as users are served in a fraction of time, total rate achieved in ST is higher. On the contrary, with long-

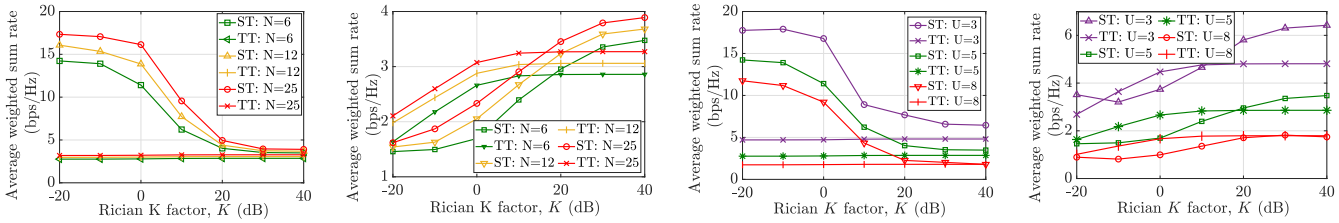

(a) (b) (c) (d)

Fig. 4: Average weighted sum rate performance of joint beamforming for different number of (a) transmit antennas with CSI, (b) transmit antennas with long-term channel statistics available, (c) users U with CSI available, (d) users U with long-term channel statistics.

term channel statistics, due to poor alignment of resources with instantaneous channel conditions, $\gamma_u^s < \gamma_u^t$ due to insufficient interference cancellation. Thus, individual user SINR guarantee is higher in TT than ST in general, thereby enhancing the sum rates in TT. However, at high K values, the channel is governed by statistically identical LOS paths, resulting in two users being served with a higher SINR guarantee, both with CSI and under long-term channel statistics. ST may or may not outperform TT depending on the interference cancellation level at each user governed by number of users being served.

The performance of ST may increase or decrease with K, depending on the type of beamforming and CSI availability. However, for TT weighted sum rate increases and then saturates at high K. This is because TT makes multi-user scenario single user thereby operating in interference free channel. The crossover between TT and ST solely depends on the system and channel parameters. With CSI available, ST gives on an average 154% and 233% gains with respect to TT for phase and joint beamforming, respectively. However, with long-term channel statistics, TT outperforms ST on an average by 56% and 2.9% for phase and joint beamforming, respectively.

Remark 7. *For ST and TT the additional gains in joint beamforming with respect to only phase beamforming results from the enhanced interference reduction achieved by the virtue of polarization synchronization.*

3) Impact of CSI at the transmitter: Fig. 3(a) shows that at low K values, higher gains are obtained with CSI (e.g., at $K = -10$ dB, CSI availability offers 89.24% gain over long-term channel statistics for ST). These high gains are obtained due to the resource allocation in every coherence interval. This aspect is compounded by the channel diversity which enhance the overall system performance. However, without CSI the resource optimization is based on the channel statistics, such as mean and variance. Consequently, the allocated resources might not closely align with the instantaneous channel conditions for the allocated window, causing degradation in weighted sum rate. At high K values, channel instances are close to the mean values. Hence, performance with CSI and with only long-term channel statistics are same for both ST and TT. On average, with CSI, ST (and TT) offers 72% (and 15%) and 56% (and 14%) gain over long-term channel statistics for phase beamforming and joint beamforming, respectively.

4) Verification of theoretical and simulation results: In this subsection, we validate the theoretical analysis and simulation performance in Fig. 3(b) with long-term channel statistics. For ST, we observe that the simulation closely matches with theory with normalized root mean square error (NRMSE) of 0.005 and 0.0083 for phase and joint beamforming, respectively, thus confirming the accuracy of the analytical model. For TT, upper bound for average weighted sum rate as stated in (56) is verified. We observe that for $K > 0$ dB bound is tight with the difference of $\approx 0.58\%$ and 0.104% for joint and phase beamforming respectively. However for low K values, bound is loose as difference increases, leading to 7.37% and 6.06% at $K = -10$ dB for phase and joint beamforming, respectively.

Remark 8. *With CSI available at the transmitter, links from base station to each user behave independently with each other, thus providing new sort of diversity thereby enhancing the overall system performance at low Rician K-factors.*

C. Impact of N and U on Joint Beamforming in Multiaccess

1) Impact of number of transmit antennas, N: Figs. 4(a) and 4(b) capture the impact of N on joint beamforming with CSI and only long-term channel statistics, respectively. As N increases, the performance of both ST and TT improve which can be attributed to the additional beamforming gains offered by the increase in number of transmit antennas. With CSI, the level of improvement decreases with increase in K for ST. For example, at $K = -10$ and 30 dB, 28% and 12% respectively, improvement is observed on increasing N from 6 to 25. However, with long-term channel statistics, the level of improvement increases with K and gets approximately saturated at high K. In both cases, the improvement is governed by the interference level observed by the users. For TT, performance improvement is roughly identical for all K values, as it is interference-free and solely governed by beamforming gain.

2) Impact of number of users, U: Fig. 4(c) and 4(d) show the joint beamforming performance variation with U with CSI and long-term channel statistics available at the transmitter, respectively. Performance degrades with increase in U due to increased interference, which is intuitive. Additionally, as U increases, the gains observed by ST over TT decrease for all the Rician K values for both cases. Moreover, increasing the number of users decreases the K factor range over which ST outperforms TT. This is because with the addition of each user, the probability of each user attaining orthogonality resulting from destructive phase and polarization interference reduces.

D. Impact of Transmit Power P_t on Beamforming Strategies

Figs. 5(a) and 5(b) capture the impact of P_t for different K values with CSI and only long-term channel statistics, respec-

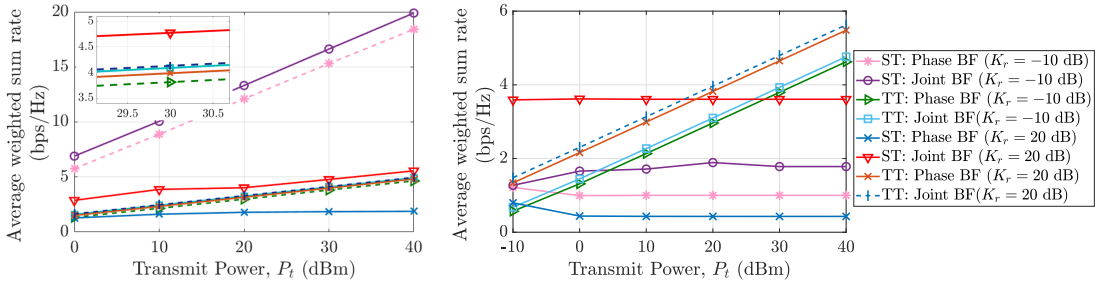

(a) (b)

Fig. 5: Variation of weighted sum rate with transmit power P_t with (a) CSI available, (b) long-term channel statistics; BF: beamforming.

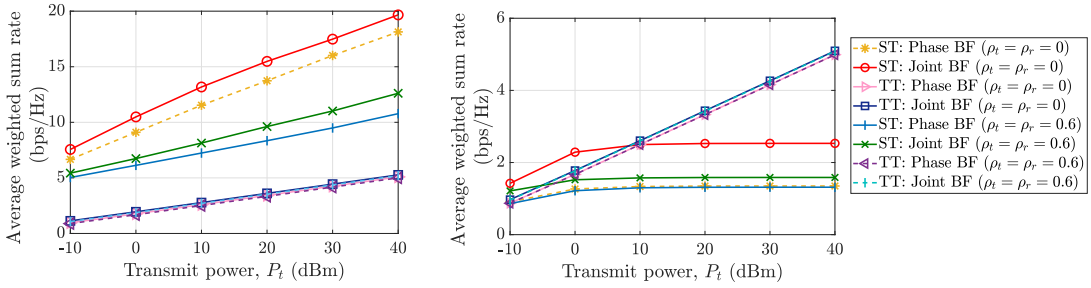

(a) (b)

Fig. 6: Impact of correlation on weighted sum rate performance with (a) CSI available, (b) long-term channel statistics; BF: beamforming.

tively. Simulation parameters: $U = 4$, $N = 10$, $\gamma_{th} = -15$ dB. For TT, weighted sum rate increases with P_t for both phase and joint beamforming, which is also evident from (46). However for ST, with CSI the performance is observed to increase in the operating range of P_t for joint beamforming due to independent resource allocation in every coherence interval, and the improvement level depends on K values. With long-term channel statistics, in the considered range of P_t, ST and TT are observed to outperform one another as K changes. Polarization alignment on top of phase alignment increases P_t over which ST outperforms TT. This is because increasing P_t also increases the interference power along with signal power. Thus, at large P_t weighted sum rates tend to decrease. This behavior is evident in Fig. 5(b) for $K = -10$ dB where after 20 dB weighted sum rate decreases for joint beamforming.

E. Impact of Spatial Correlation on Beamforming Strategies

In the results so far correlation parameters have been taken to be zero. In the following, we take finite correlation values and compare the results with the uncorrelated scenario. Simulations are carried out for $U = 4$, $N = 12$, $\gamma_{th} = -20$ dB, and $K = 0$ dB. As evident from Fig. 6(a) and 6(b), increasing the transmit and receive channel spatial correlation actually degrades the weighted sum rate performance.

With CSI available at the transmitter and correlation of 0.6, gains with joint beamforming in comparison to phase beamforming are $\approx 13\%$ and $\approx 9\%$ for ST and TT, respectively. However, without correlation, corresponding gains are $\approx 12\%$ and 8%, respectively. Thus, transmit and receive correlation as high as 0.6 lightly impact the gains offered by joint beamforming over phase beamforming for ST and TT scenarios. Additionally, we observe that, ST outperforms TT for all considered transmit powers when CSI is available.

With long-term channel statistics, improvement in joint beamforming with respect to phase beamforming is reduced from $\approx 80\%$ to $\approx 24\%$ with correlation of 0.6 for ST. We observe that joint beamforming is more affected due to spatial correlation compared to phase beamforming as the benefits of both phase and polarization orthogonality offered by the channel reduces. However, for TT no degradation is observed as resource allocation is based on the average channel. Though the gains are reduced, joint beamforming in spatially correlated channels still offers improvement over phase beamforming. The transmit power levels over which ST outperforms TT decrease due to degraded interference cancellation.

Remark 9. *Polarization synchronization provides additional gain over only phase alignment. The gain quantity may differ based on single user or multi-user scenario and the type of communication technique employed.*

F. Impact of XPD on Beamforming Strategies

Fig. 7 shows the impact of XPD on weighted sum rate performance. XPD measures the polarization leakage between the orthogonal signal components. Fig. 7(a) shows that when CSI is available at the transmitter, XPD has negligible impact on the performance. For ST, this is due to the sufficient interference cancellation by the virtue of channel diversity. For TT, as single user is served at a time there exists no inter-user interference, XPD does not affect the sum rate. Overall, with CSI available, XPD only redistributes power between the two orthogonal components. However, as resources are allocated based on instantaneous channel, the impact is negligible.

Fig. 7(b) shows the performance with long-term channel statistics. In this case, poor alignment of resources with the instantaneous channel conditions causes insufficient interference

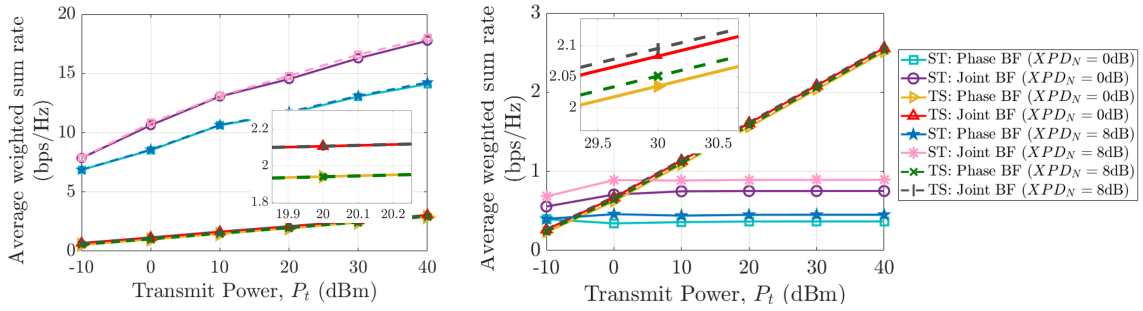

(a) (b)

Fig. 7: Performance of XPD with transmit power P_t with (a) CSI available, (b) long-term channel statistics; BF: beamforming.

cancellation for ST. Thus, performance improves with XPD due to enhanced interference cancellation. For TT performance is negligibly affected due to no inter-user interference. Slight difference in performance is observed due to polarization leakage which is more pronounced with channel statistics.

G. Impact of Proposed Beamforming Strategies on NOMA

In this subsection, we show the performance enhancement of the existing multiaccess scheme through joint beamforming. We select NOMA as an example case of ST. We consider that user 1 is allocated maximum power (and hence cannot decode interfering signals), while user U is the allocated least power and is able to nullify interference from all other users by performing successive interference cancellation (SIC). The achievable rate after SIC operation at the u^{th} user to decode the message of k^{th} user with $k < u, \forall\ k = 1, 2, ..., (u-1)$ is

$$R_{u\to k} = \log_2\left(1 + \frac{|\mathbf{q}_u^H \mathbf{H}_u \mathbf{P}_k \mathbf{F}_k|^2}{\sum_{j=u+1}^{U} |\mathbf{q}_u^H \mathbf{H}_u \mathbf{P}_j \mathbf{F}_j|^2 + \sigma_0^2}\right). \quad (57)$$

The weighted sum rate optimization for NOMA is given as

$$(\text{P8}): \max_{\mathbf{F},\mathbf{P}} \quad R_N = \sum_{u=1}^{U} \beta_u R_{u\to u} \quad (58a)$$

$$\text{s.t.} \quad R_{k\to u} \geq R_{u\to u} \quad \forall u < k, \ \forall k \quad (58b)$$

$$(30b),\ (32)\ \text{and}\ (18c).$$

(58b) is the SIC feasibility constraint for NOMA which ensures that u^{th} user must decode k^{th} user's message with a rate no smaller than that experienced by the k^{th} user itself. Objective in (58a) and the constraint (58b) are non-convex and (P8) is NP-hard. The constraint (58b) can be rewritten as

$$\gamma_{k\to u} \geq \gamma_{u\to u} \quad \forall\ u < k, \forall k \quad (59)$$

where $\gamma_{k\to u} = 2^{R_{k\to u}}$. To ensure this constraint we enforce a sufficient condition given by

$$\gamma_{k\to u} \geq \gamma_{th}^s, \quad \gamma_{u\to u} \geq \gamma_{th}^s. \quad (60)$$

It can be equivalently reformulated as a second-order cone constraint and efficiently handled by SOCP. With CSI available at the transmitter $\mathbb{E}[\gamma_u^s] = \gamma_u^s$ and with long-term channel statistics if $\gamma_u^s \geq \gamma_{th}^s$ for every channel instance, then (18c) is also satisfied. We observe that minimum SINR constraint (18c) and SIC constraint (60) are linked. To convexify optimization problem, we revise (P8) using the WMMSE framework as

$$(\text{P9}): \max_{\mathbf{P},\mathbf{F},\mathbf{b}^z,\mathbf{a}^z} \quad \sum_{u=1}^{U} \beta_u^z (b_u^z e_u^z - \log_2 b_u^z) \quad (61a)$$

$$\text{s.t.} \quad (30b),\ (32)\ \text{and}\ (60)$$

where $\mathbf{e}^c$, $\mathbf{a}^c$, and $\mathbf{b}^c$ can be computed using the similar steps as used in computing (20), (22) and (23). Similarly, $\mathbf{e}^l$, $\mathbf{a}^l$, and $\mathbf{b}^l$ can be computed using the similar steps as used in computing (25), (27) and (28). We follow the similar strategy of alternate optimization as used in Section III to obtain optimal values of $\mathbf{P}$ and $\mathbf{F}$. To compute the results with phase beamforming for NOMA, $\mathbf{P}$ is replaced with $\mathbf{W}$ and $\mathbf{F}$ is replaced with $\mathbf{T}$ and an initialized value of $\mathbf{T}$ is used throughout the algorithm.

Next, we compare the performance of NOMA-based ST with phase and joint beamforming. Simulation parameters are: $U = 3$, $N = 10$, and $\gamma_{th} = -20$ dB. Fig. 8(a) and 8(b) show that joint beamforming outperforms phase beamforming, and the level of improvement depends on K values. At low K, with CSI available, phase beamforming in itself is capable of exploiting the channel diversity thus giving small improvement through polarization beamforming. However, at high K as higher power is in the direct component, small misalignment in polarization heavily degrades the performance. Thus, joint beamforming gives higher gains over phase beamforming. However, with long-term channel statistics, lesser gains are observed at low K values due to poor alignment of resources with instantaneous channel conditions. At high K statistically identical paths allows polarization beamforming to give enhanced gains due to improved interference cancellation.

H. Impact of Imperfect CSI on Beamforming Strategies

In the analysis and the results so far we have either considered perfect CSI or long-term channel statistics at the transmitter. However in realistic wireless scenarios, channel CSI is estimated and is known imperfectly. Thus, we also analyze the impact of imperfect CSI on phase and joint beamforming. The relation between the perfect and imperfect CSI can be expressed as [44], [45]

$$\mathbf{H}_{un} = \sqrt{1-\chi_{un}}\bar{\mathbf{H}}_{un} + \sqrt{\chi_{un}}\mathbf{E}_{un}. \quad (62)$$

$\mathbf{H}_{un}$ is the true channel between the n^{th} dual-polarized transmit antenna and u^{th} user. $\bar{\mathbf{H}}_{un}$ is the corresponding imperfect

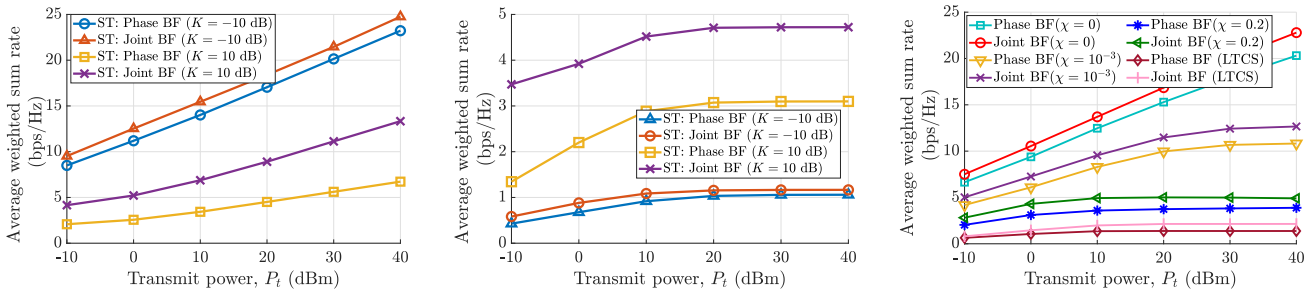

(a) (b) (c)

Fig. 8: (a) Performance of NOMA-based ST with CSI available, (b) Performance of NOMA-based ST with long-term channel statistics, (c) Impact of imperfect CSI on ST; BF: beamforming, LTCS: long-term channel statistics.

channel. $\mathbf{E}_{un}$ is the error matrix with i.i.d. zero-mean and unit-variance complex Gaussian entries independent of $\bar{\mathbf{H}}_{un}$. $\chi_{un} \in [0\ 1]$, characterizes partial CSI since $\chi_{un} = 0$ corresponds to perfect CSI and $\chi_{un} = 1$ corresponds to no CSI knowledge.

Fig. 8(c) captures the impact of imperfect CSI through χ. Simulation parameters are: $U = 4$, $N = 10$, $K = -10$ dB, and $\gamma_{th} = -20$ dBm. For brevity, we present the results for ST. We consider equal χ for all the channels. We observe that with imperfect CSI, the designed beamformers cannot perfectly suppress interference. At low transmit power levels, we observe small impact on weighted sum rate. This is because the system is noise-limited and the residual interference from CSI errors is small. At high transmit power levels, system becomes interference-limited. Thus, the residual interference does not vanish, thereby saturating the weighted sum rate. Note that similar performance can be observed for TT.

VI. Conclusion

In this paper, it was established that joint phase and polarization synchronization is necessary for maximized gains irrespective of the channel and system conditions. Two alternative transmission mechanisms: ST and TT in presence of CSI as well as with only long-term channel statistics were utilized to demonstrate the benefits of joint beamforming over only phase beamforming. The level of improvement obtained by joint beamforming was shown to depend on relative mismatch between the polarization of desired and undesired symbol and receiver polarization in ST. Thus, in ST both polarization beamforming and nullforming play an important role in performance improvement. However in TT, the performance only depends on the relative polarization mismatch between the transmitter and receiver as it orthogonalizes the multi-user transmissions. Additionally, it was noted that LOS strength, CSI availability, transmit power level, and SINR threshold impact the choice of the multiaccess transmission for improved gains. To capture real wireless scenarios, performance of ST with imperfect CSI was also analyzed. Performance studies revealed that, due to diversity provided by the LOS strength, optimal resource allocation should utilize CSI; however, with strong LOS, long-term channel statistics could be preferred due to its low computational complexity as the performance with CSI and long-term channel statistics are similar. Performance benefits of the proposed joint beamforming strategies were also shown using NOMA as an example case.

Appendix

A. *Proof of Lemma* 1

We first compute the term $\mathbf{q}_u^H \mathbf{H}_u \mathbf{P}_j \mathbf{F}_j$ for two transmit antennas, i.e. $N = 2$.

$$\begin{aligned}\mathbf{q}_u^H \mathbf{H}_u \mathbf{P}_j \mathbf{F}_j =& \mathbf{q}_u^H \begin{bmatrix}\mathbf{H}_{u1} & \mathbf{H}_{u2}\end{bmatrix} \begin{bmatrix}\sqrt{p_{j1}}[\mathbf{I}_2] & [\mathbf{0}] \\ [\mathbf{0}] & \sqrt{p_{j2}}[\mathbf{I}_2]\end{bmatrix} \begin{bmatrix}\mathbf{f}_{j1} \\ \mathbf{f}_{j2}\end{bmatrix} \\ =& \mathbf{q}_u^H \left[\sqrt{p_{j1}}[\mathbf{H}_{u1}]\mathbf{f}_{j1} + \sqrt{p_{j2}}[\mathbf{H}_{u2}]\mathbf{f}_{j2}\right].\end{aligned} \tag{A.1}$$

Now substituting channel matrices, and transmitter and receiver polarization vectors, we obtain

$$\begin{aligned}\mathbf{q}_u^H \mathbf{H}_u \mathbf{P}_j \mathbf{F}_j =& \begin{bmatrix}q_u^h \\ q_u^v\end{bmatrix}^H \left(\sqrt{p_{j1}} \begin{bmatrix}h_{u1}^{hh} & h_{u1}^{hv} \\ h_{u1}^{vh} & h_{u1}^{vv}\end{bmatrix} \begin{bmatrix}f_{j1}^h \\ f_{j1}^v\end{bmatrix} + \sqrt{p_{j2}} \begin{bmatrix}h_{u2}^{hh} & h_{u2}^{hv} \\ h_{u2}^{vh} & h_{u2}^{vv}\end{bmatrix} \begin{bmatrix}f_{j2}^h \\ f_{j2}^v\end{bmatrix}\right) \\ =& \sqrt{p_{j1}} \left(q_u^{h*} h_{u1}^{hh} f_{j1}^h + q_u^{h*} h_{u1}^{hv} f_{j1}^v + q_u^{v*} h_{u1}^{vh} f_{j1}^h + q_u^{v*} h_{u1}^{vv} f_{j1}^v\right) \\ &+ \sqrt{p_{j2}} \left(q_u^{h*} h_{u2}^{hh} f_{j2}^h + q_u^{h*} h_{u2}^{hv} f_{j2}^v + q_u^{v*} h_{u2}^{vh} f_{j2}^h + q_u^{v*} h_{u2}^{vv} f_{j2}^v\right) \\ =& \underbrace{[\eta_{ju1}^{hh} h_{u1}^{hh} + \eta_{ju1}^{hv} h_{u1}^{hv} + \eta_{ju1}^{vh} h_{u1}^{vh} + \eta_{ju1}^{vv} h_{u1}^{vv}}_{n=1} \\ &+ \underbrace{\eta_{ju2}^{hh} h_{u2}^{hh} + \eta_{ju2}^{hv} h_{u2}^{hv} + \eta_{ju2}^{vh} h_{u2}^{vh} + \eta_{ju2}^{vv} h_{u2}^{vv}]}_{n=2}.\end{aligned} \tag{A.2}$$

Thus, for generalized N, it can be written as

$$\mathbf{q}_u^H \mathbf{H}_u \mathbf{P}_j \mathbf{F}_j = \sum_{n=1}^{N} [\eta_{jun}^{hh} h_{un}^{hh} + \eta_{jun}^{hv} h_{un}^{hv} + \eta_{jun}^{vh} h_{un}^{vh} + \eta_{jun}^{vv} h_{un}^{vv}] \tag{A.3}$$

where $\eta_{jun}^{hh} = \sqrt{P_{jn}} q_u^{h*} f_{jn}^h$, $\eta_{jun}^{hv} = \sqrt{P_{jn}} q_u^{h*} f_{jn}^v$, $\eta_{jun}^{vh} = P_{jn} q_u^{v*} f_{jn}^h$, and $\eta_{jun}^{vv} = \sqrt{P_{jn}} q_u^{v*} f_{jn}^v$. Splitting the terms in (A.3) into real and imaginary parts considering $\eta_{jun}^{w} = \eta_{jun}^{wr} + j\eta_{jun}^{wi}$ and $h_{un}^{w} = h_{un}^{wr} + j h_{un}^{wi}$, $w \in \mathscr{S}_3$ and solving further we get $\mathbf{q}_u^H \mathbf{H}_u \mathbf{P}_j \mathbf{F}_j = \zeta_{ju}^r + j\zeta_{ju}^i = \boldsymbol{\zeta}_{ju}^T \boldsymbol{\zeta}_{ju}$ where $\boldsymbol{\zeta}_{ju} = [\zeta_{ju}^r\ \zeta_{ju}^i]^T$, ζ_{ju}^r, and ζ_{ju}^i are respectively given by

$$\begin{aligned}\zeta_{ju}^r = \sum_{n=1}^{N} \Big[&\eta_{jun}^{hhr} h_{un}^{hhr} - \eta_{jun}^{hhi} h_{un}^{hhi} + \eta_{jun}^{hvr} h_{un}^{hvr} - \eta_{jun}^{hvi} h_{un}^{hvi} \\ &+ \eta_{jun}^{vhr} h_{un}^{vhr} - \eta_{jun}^{vhi} h_{un}^{vhi} + \eta_{jun}^{vvr} h_{un}^{vvr} - \eta_{jun}^{vvi} h_{un}^{vvi}\Big]\end{aligned} \tag{A.4}$$

$$\begin{aligned}\zeta_{ju}^i = \sum_{n=1}^{N} \Big[&\eta_{jun}^{hhi} h_{un}^{hhr} + \eta_{jun}^{hhr} h_{un}^{hhi} + \eta_{jun}^{hvi} h_{un}^{hvr} + \eta_{jun}^{hvr} h_{un}^{hvi} \\ &+ \eta_{jun}^{vhi} h_{un}^{vhr} + \eta_{jun}^{vhr} h_{un}^{vhi} + \eta_{jun}^{vvi} h_{un}^{vvr} + \eta_{jun}^{vvr} h_{un}^{vvi}\Big].\end{aligned} \tag{A.5}$$

Next, we compute the mean and variance for ζ_{ju}^r and ζ_{ju}^i. Using (1), (5) and (10), we first compute the individual channel coefficients of $\mathbf{H}_{un}$ in terms of channel parameters given as

$$h_{un}^{hh} = \xi_u\sqrt{\frac{K(1-\alpha_L)}{1+K}}\tilde{g}_{un}^{hh} + \xi_u\left[\sqrt{\frac{1-\alpha_N}{1+K}}\sum_{p=1}^{U}\sum_{q=1}^{N} \{\delta_{up}^{hh}(\hat{g}_{pq}^{hh}\rho_{qn}^{hh} + \hat{g}_{pq}^{hv}\rho_{qn}^{vh}) + \delta_{up}^{hv}(\hat{g}_{pq}^{vh}\rho_{qn}^{hh} + \hat{g}_{pq}^{vv}\rho_{qn}^{vh})\}\right] \tag{A.6}$$

$$h_{un}^{hv} = \xi_u\sqrt{\frac{K\alpha_L}{1+K}}\tilde{g}_{un}^{hv} + \xi_u\left[\sqrt{\frac{\alpha_N}{1+K}}\sum_{p=1}^{U}\sum_{q=1}^{N} \{\delta_{up}^{hh}(\hat{g}_{pq}^{hh}\rho_{qn}^{hv} + \hat{g}_{pq}^{hv}\rho_{qn}^{vv}) + \delta_{up}^{hv}(\hat{g}_{pq}^{hh}\rho_{qn}^{hv} + \hat{g}_{pq}^{hv}\rho_{qn}^{vv})\}\right] \tag{A.7}$$

$$h_{un}^{vh} = \xi_u\sqrt{\frac{K\alpha_L}{1+K}}\tilde{g}_{un}^{vh} + \xi_u\left[\sqrt{\frac{\alpha_N}{1+K}}\sum_{p=1}^{U}\sum_{q=1}^{N} \{\delta_{up}^{vh}(\hat{g}_{pq}^{hh}\rho_{qn}^{hh} + \hat{g}_{pq}^{hv}\rho_{qn}^{vh}) + \delta_{up}^{vv}(\hat{g}_{pq}^{vh}\rho_{qn}^{hh} + \hat{g}_{pq}^{vv}\rho_{qn}^{vh})\}\right] \tag{A.8}$$

$$h_{un}^{vv} = \xi_u\sqrt{\frac{K(1-\alpha_L)}{1+K}}\tilde{g}_{un}^{vv} + \xi_u\left[\sqrt{\frac{1-\alpha_N}{1+K}}\sum_{p=1}^{U}\sum_{q=1}^{N} \{\delta_{up}^{vh}(\hat{g}_{pq}^{hh}\rho_{qn}^{hv} + \hat{g}_{pq}^{hv}\rho_{qn}^{vv}) + \delta_{up}^{vv}(\hat{g}_{pq}^{vh}\rho_{qn}^{hv} + \hat{g}_{pq}^{vv}\rho_{qn}^{vv})\}\right] \tag{A.9}$$

where we have used the substitutions

$$(\mathbf{C}_t)^{\frac{1}{2}} = \begin{bmatrix} [\rho_{11}] & [\rho_{12}] & \cdots & [\rho_{1N}] \\ [\rho_{21}] & [\rho_{22}] & \cdots & [\rho_{2N}] \\ . & . & \cdots & . \\ [\rho_{N1}] & [\rho_{N2}] & \cdots & [\rho_{NN}] \end{bmatrix} \in \mathbb{C}^{2N\times 2N} \tag{A.10}$$

$$(\mathbf{C}_r)^{\frac{1}{2}} = \begin{bmatrix} [\delta_{11}] & [\delta_{12}] & \cdots & [\delta_{1U}] \\ [\delta_{21}] & [\delta_{22}] & \cdots & [\delta_{2U}] \\ . & . & \cdots & . \\ [\delta_{U1}] & [\delta_{U2}] & \cdots & [\delta_{UU}] \end{bmatrix} \in \mathbb{C}^{2U\times 2U} \tag{A.11}$$

where each element is a block diagonal matrix such that

$$\rho_{n_1n_2} = \begin{bmatrix} \rho_{n_1n_2}^{hh} & \rho_{n_1n_2}^{hv} \\ \rho_{n_1n_2}^{vh} & \rho_{n_1n_2}^{vv} \end{bmatrix} \text{ and } \delta_{n_1n_2} = \begin{bmatrix} \delta_{u_1u_2}^{hh} & \delta_{u_1u_2}^{hv} \\ \delta_{u_1u_2}^{vh} & \delta_{u_1u_2}^{vv} \end{bmatrix}. \tag{A.12}$$

h_{un}^{wr} and h_{un}^{wi} can be obtained from (A.6)-(A.9) by substituting $\hat{g}_{pq}^{w} = \hat{g}_{pq}^{wr} + \hat{g}_{pq}^{wi}$ and separating the real and imaginary parts. Thus, real and imaginary parts of the channel coefficients can be expressed as

$$h_{un}^{hhd} = \xi_u\sqrt{\frac{K(1-\alpha_L)}{1+K}}\tilde{g}_{un}^{hhd} + \xi_u\sqrt{\frac{1-\alpha_N}{1+K}}\sum_{p=1}^{U}\sum_{q=1}^{N} \{\delta_{up}^{hh}(\hat{g}_{pq}^{hhd}\rho_{qn}^{hh} + \hat{g}_{pq}^{hvd}\rho_{qn}^{vh}) + \delta_{up}^{hv}(\hat{g}_{pq}^{vhd}\rho_{qn}^{hh} + \hat{g}_{pq}^{vvd}\rho_{qn}^{vh})\} \tag{A.13}$$

$$h_{un}^{hvd} = \xi_u\sqrt{\frac{K\alpha_L}{1+K}}\tilde{g}_{un}^{hvd} + \xi_u\sqrt{\frac{\alpha_N}{1+K}}\sum_{p=1}^{U}\sum_{q=1}^{N} \{\delta_{up}^{hh}(\hat{g}_{pq}^{hhd}\rho_{qn}^{hv} + \hat{g}_{pq}^{hvd}\rho_{qn}^{vv}) + \delta_{up}^{hv}(\hat{g}_{pq}^{vhd}\rho_{qn}^{hv} + \hat{g}_{pq}^{vvd}\rho_{qn}^{vv})\} \tag{A.14}$$

$$h_{un}^{vhd} = \xi_u\sqrt{\frac{K\alpha_L}{1+K}}\tilde{g}_{un}^{vhd} + \xi_u\sqrt{\frac{\alpha_N}{1+K}}\sum_{p=1}^{U}\sum_{q=1}^{N} \{\delta_{up}^{vh}(\hat{g}_{pq}^{hhd}\rho_{qn}^{hh} + \hat{g}_{pq}^{hvd}\rho_{qn}^{vh}) + \delta_{up}^{vv}(\hat{g}_{pq}^{vhd}\rho_{qn}^{hh} + \hat{g}_{pq}^{vvd}\rho_{qn}^{vh})\} \tag{A.15}$$

$$h_{un}^{vvd} = \xi_u\sqrt{\frac{K(1-\alpha_L)}{1+K}}\tilde{g}_{un}^{vvd} + \xi_u\sqrt{\frac{1-\alpha_N}{1+K}}\sum_{p=1}^{U}\sum_{q=1}^{N} \{\delta_{up}^{vh}(\hat{g}_{pq}^{hhd}\rho_{qn}^{hv} + \hat{g}_{pq}^{hvd}\rho_{qn}^{vv}) + \delta_{up}^{vv}(\hat{g}_{pq}^{vhd}\rho_{qn}^{hv} + \hat{g}_{pq}^{vvd}\rho_{qn}^{vv})\} \tag{A.16}$$

where $d \in \mathscr{S}_5$. As $\hat{g}_{pq}^{w} \sim \mathscr{CN}(0,1)$, each term in ζ_{ju}^r and ζ_{ju}^i are independent and Gaussian distributed. By central limit theorem $\zeta_{ju}^r \sim \mathscr{CN}(\mu_{\zeta_{ju}^r}, \sigma_{\zeta_{jn}^r}^2)$ and $\zeta_{ju}^i \sim \mathscr{CN}(\mu_{\zeta_{ju}^i}, \sigma_{\zeta_{jn}^i}^2)$.

$$\mu_{\zeta_{ju}^r} = \sum_{n=1}^{N} \eta_{jun}^{hhi}\mathbb{E}[h_{un}^{hhr}] + \eta_{jun}^{hvi}\mathbb{E}[h_{un}^{hvr}] + \eta_{jun}^{vhi}\mathbb{E}[h_{un}^{vhr}] + \eta_{jun}^{vvi}\mathbb{E}[h_{un}^{vvr}] \tag{A.17}$$

$$\mu_{\zeta_{ju}^i} = \sum_{n=1}^{N} \eta_{jun}^{hhi}\mathbb{E}[h_{un}^{hhr}] + \eta_{jun}^{hvi}\mathbb{E}[h_{un}^{hvr}] + \eta_{jun}^{vhi}\mathbb{E}[h_{un}^{vhr}] + \eta_{jun}^{vvi}\mathbb{E}[h_{un}^{vvr}] \tag{A.18}$$

where we have used $\mathbb{E}[h_{un}^{hhi}] = \mathbb{E}[h_{un}^{vvi}] = \mathbb{E}[h_{un}^{hvi}] = \mathbb{E}[h_{un}^{vhi}] = 0$. Substituting $\mathbb{E}[h_{un}^{hhr}] = \mathbb{E}[h_{un}^{vvr}] = \sqrt{\frac{K(1-\alpha_L)}{1+K}}$ and $\mathbb{E}[h_{un}^{hvr}] = \mathbb{E}[h_{un}^{vhr}] = \sqrt{\frac{K\alpha_L}{1+K}}$, we obtain (41) and (42) respectively. Using (A.4), (A.5), and (A.13)-(A.16) we compute $\sigma_{\zeta_{jn}^r}^2$ and $\sigma_{\zeta_{jn}^i}^2$ and observe that $\sigma_{\zeta_{jn}^r}^2 = \sigma_{\zeta_{jn}^i}^2 = \sigma_{\zeta_{jn}}^2$, which is defined in (43) with $\delta_{up}^h = (\delta_{up}^{hh})^2 + (\delta_{up}^{hv})^2$, $\delta_{up}^v = (\delta_{up}^{vh})^2 + (\delta_{up}^{vv})^2$, $\delta_{up}^t = \{\delta_{up}^{vh}\delta_{up}^{hh} + \delta_{up}^{vv}\delta_{up}^{hv}\}$, $\rho_{qmn}^a = \{\rho_{qn}^{hv}\rho_{qm}^{hv} + \rho_{qn}^{vv}\rho_{qm}^{vv}\}$, $\rho_{qmn}^b = \{\rho_{qn}^{hh}\rho_{qm}^{hh} + \rho_{qn}^{vh}\rho_{qm}^{vh}\}$, $\rho_{qmn}^c = \{\rho_{qn}^{hh}\rho_{qm}^{hv} + \rho_{qn}^{vh}\rho_{qm}^{vv}\}$, and $\rho_{qmn}^d = \{\rho_{qn}^{hv}\rho_{qm}^{hh} + \rho_{qn}^{vv}\rho_{qm}^{vh}\}$. Accordingly, $\boldsymbol{\zeta}_{ju}$ is bivariate Gaussian distributed.

B. Proof of Lemma 2

To compute $\mathbb{E}[\boldsymbol{\zeta}_{ju}^T\boldsymbol{\zeta}_{ju}]$, we use moment generating function of the bivariate Gaussian distribution which is

$$\Phi_{\zeta_{ju}}(\boldsymbol{t}) = \exp\left(\boldsymbol{\mu}_{\zeta_{ju}}^T\boldsymbol{t} + \frac{1}{2}t^T\boldsymbol{C}_{\zeta_{ju}}\boldsymbol{t}\right). \tag{B.1}$$

Taking first and second order derivatives of $\Phi_{\zeta_{ju}}(\boldsymbol{t})$ we get

$$\begin{aligned} \frac{\partial\Phi_{\zeta_{ju}}(t)}{\partial t} &= \left(\boldsymbol{\mu}_{\zeta_{ju}} + \boldsymbol{C}_{\zeta_{ju}}\boldsymbol{t}\right)\Phi_{\zeta_{ju}} \\ \frac{\partial^2\Phi_{\zeta_{ju}}(t)}{\partial t^2} &= \boldsymbol{C}_{\zeta_{ju}}\Phi_{\zeta_{ju}} + \left(\boldsymbol{\mu}_{ju} + \boldsymbol{C}_{\zeta_{ju}}\boldsymbol{t}\right)\left(\boldsymbol{\mu}_{\zeta_{ju}} + \boldsymbol{C}_{\zeta_{ju}}\boldsymbol{t}\right)^T\Phi_{\zeta_{ju}} \end{aligned} \tag{B.2}$$

$$\begin{aligned} \mathbb{E}[\boldsymbol{\zeta}_{ju}^T\boldsymbol{\zeta}_{ju}] &= \text{Tr}\left[\frac{\partial^2\Phi_{\zeta_{ju}}}{\partial t^2}\bigg|_{t=0}\right] = \text{Tr}\left[\boldsymbol{C}_{\zeta_{ju}} + \boldsymbol{\mu}_{\zeta_{ju}}\boldsymbol{\mu}_{\zeta_{ju}}^T\right] \\ &= (2\sigma_{\zeta_{ju}}^2 + \mu_{\zeta_{ju}^r}^2 + \mu_{\zeta_{ju}^i}^2). \end{aligned} \tag{B.3}$$

Next we compute $\mathbb{E}[\mathbf{q}_u^H\mathbf{H}_u\mathbf{P}_j\mathbf{F}_j]$ for $N = 2$ case, we get

$$\begin{aligned} &\mathbb{E}\left[\mathbf{q}_u^H\mathbf{H}_u\mathbf{P}_j\mathbf{F}_j\right] = \mathbf{q}_u^H\mathbb{E}[\left[\sqrt{p_{j1}}\mathbf{H}_{u1}\mathbf{f}_{j1} + \sqrt{p_{j2}}\mathbf{H}_{u2}\mathbf{f}_{j2}\right]\Big] \\ &= \underbrace{[\eta_{ju1}^{hh}\mathbb{E}[h_{u1}^{hh}] + \eta_{ju1}^{hv}\mathbb{E}[h_{u1}^{hv}] + \eta_{ju1}^{vh}\mathbb{E}[h_{u1}^{vh}] + \eta_{ju1}^{vv}\mathbb{E}[h_{u1}^{vv}]}_{n=1} \\ &+ \underbrace{\eta_{ju2}^{hh}\mathbb{E}[h_{u2}^{hh}] + \eta_{ju2}^{hv}\mathbb{E}[h_{u2}^{hv}] + \eta_{ju2}^{vh}\mathbb{E}[h_{u2}^{vh}] + \eta_{ju2}^{vv}\mathbb{E}[h_{u2}^{vv}]]}_{n=2}. \end{aligned} \tag{B.4}$$

In general the above expression can be written as

$$\begin{aligned} \mathbb{E}[\mathbf{q}_u^H\mathbf{H}_u\mathbf{P}_j\mathbf{F}_j] = \sqrt{\frac{K}{1+K}}\xi_u\sum_{n=1}^{N}\Big[&(\eta_{jun}^{hh} + \eta_{jun}^{vv})\sqrt{1-\alpha_L} \\ &+ (\eta_{jun}^{hv} + \eta_{jun}^{vh})\sqrt{\alpha_L}\Big]. \end{aligned} \tag{B.5}$$

Substituting (B.3) and (B.5) in (44) we obtain Lemma 2.

REFERENCES

[1] A. F. M. S. Shah, M. A. Karabulut, and K. Rabie, "Multiple access schemes for 6G enabled NTN-assisted IoT technologies: Recent developments, prospects and challenges," *IEEE Internet Things J.*, vol. 7, no. 1, pp. 48–54, Jan. 2024.

[2] B. Clerckx, Y. Mao, Z. Yang, M. Chen, A. Alkhateeb, L. Liu, M. Qiu, J. Yuan, V. W. S. Wong, and J. Montojo, "Multiple access techniques for intelligent and multifunctional 6G: Tutorial, survey, and outlook," *Proc. IEEE*, vol. 112, no. 7, pp. 832–879, Jan. 2024.

[3] X. Lyu, S. Aditya, J. Kim, and B. Clerckx, "Rate-splitting multiple access: The first prototype and experimental validation of its superiority over SDMA and NOMA," *IEEE Trans. Wirel. Commun.*, vol. 23, no. 8, pp. 9986–10 000, Mar. 2024.

[4] E. A. Jorswieck, P. Svedman, and B. Ottersten, "Performance of TDMA and SDMA based opportunistic beamforming," *IEEE Trans. Wirel. Commun.*, vol. 7, no. 11, pp. 4058–4063, Dec. 2008.

[5] I. Koutsopoulos and L. Tassiulas, "The impact of space division multiplexing on resource allocation: a unified treatment of TDMA, OFDMA and CDMA," *IEEE Trans. Commun.*, vol. 56, no. 2, pp. 260–269, 2008.

[6] F. Alavi, K. Cumanan, Z. Ding, and A. G. Burr, "Beamforming techniques for nonorthogonal multiple access in 5G cellular networks," *IEEE Trans. Veh. Technol.*, vol. 67, no. 10, pp. 9474–9487, Jul. 2018.

[7] M. Sadek, A. Tarighat, and A. H. Sayed, "A leakage-based precoding scheme for downlink multi-user MIMO channels," *IEEE Trans. Wirel. Commun.*, vol. 6, no. 5, pp. 1711–1721, May 2007.

[8] A. Sousa de Sena, D. Benevides da Costa, Z. Ding, and P. H. J. Nardelli, "Massive MIMO–NOMA networks with multi-polarized antennas," *IEEE Trans. Wirel. Commun.*, vol. 18, no. 12, pp. 5630–5642, Sept. 2019.

[9] B. Hochwald, C. Peel, and A. Swindlehurst, "A vector-perturbation technique for near-capacity multiantenna multiuser communication-part II: perturbation," *IEEE Trans. Commun.*, vol. 53, no. 3, pp. 537–544, Apr. 2005.

[10] W. Yu and T. Lan, "Transmitter optimization for the multi-antenna downlink with per-antenna power constraints," *IEEE Trans. Signal Process.*, vol. 55, no. 6, pp. 2646–2660, May 2007.

[11] S. Yang, Y. Xiao, J. Chen, and P. Xiao, "Integrated polarization and spatial modulation," *IEEE Trans. Commun.*, vol. 71, no. 1, pp. 527–539, Nov. 2023.

[12] I. A. Hemadeh, P. Xiao, Y. Kabiri, L. Xiao, V. Fusco, and R. Tafazolli, "Polarization modulation design for reduced RF chain wireless," *IEEE Trans. Commun.*, vol. 68, no. 6, pp. 3890–3907, Mar. 2020.

[13] F. Wang, J. Yu, Y. Wang, W. Li, B. Zhu, J. Ding, K. Wang, C. Liu, C. Wang, M. Kong, L. Zhao, F. Zhao, and W. Zhou, "Delivery of polarization-division-multiplexing wireless millimeter-wave signal over 4.6-km at W-band," *J. Light. Technol.*, vol. 40, no. 19, pp. 6339–6346, Aug. 2022.

[14] G. Zafari, M. Koca, and H. Sari, "Dual-polarized spatial modulation over correlated fading channels," *IEEE Trans. Commun.*, vol. 65, no. 3, pp. 1336–1352, Dec. 2017.

[15] J. He, Y. Wang, T. Shu, and T.-K. Truong, "Polarization, angle, and delay estimation for tri-polarized systems in multipath environments," *IEEE Trans. Wireless Commun.*, vol. 21, no. 8, pp. 5828–5841, Jan. 2022.

[16] H. Asplund, J.-E. Berg, F. Harrysson, J. Medbo, and M. Riback, "Propagation characteristics of polarized radio waves in cellular communications," in *Proc. IEEE VTC*, Sep. 2007, pp. 839–843.

[17] C. Qian, X. Fu, N. D. Sidiropoulos, and Y. Yang, "Tensor-based channel estimation for dual-polarized massive MIMO systems," *IEEE Trans. Signal Process.*, vol. 66, no. 24, pp. 6390–6403, Oct. 2018.

[18] L. Dongwei, M. Jiazhi, W. Zhanling, and S. Longfei, "Phase-only beamforming for dual-polarization array radar based on manifold optimization," *IEEE Antennas Wirel. Propag. Lett.*, vol. 24, no. 7, pp. 1984–1988, Mar. 2025.

[19] Y. Han, X. Li, W. Tang, S. Jin, Q. Cheng, and T. J. Cui, "Dual-polarized RIS-assisted mobile communications," *IEEE Trans. Wirel. Commun.*, vol. 21, no. 1, pp. 591–606, Jul. 2022.

[20] Z. Zheng, H. Huang, H. Zhang, and A. L. Swindlehurst, "RIS-aided dual-polarized MIMO: How large a surface is needed to beat single polarization?" *IEEE Commun. Lett.*, vol. 29, no. 1, pp. 150–154, 2025.

[21] H. Bolcskei, R. Nabar, V. Erceg, D. Gesbert, and A. Paulraj, "Performance of spatial multiplexing in the presence of polarization diversity," in *Proc. IEEE Int. Conf. Acoust. Speech Signal Process.*, vol. 4, Aug. 2001, pp. 2437–2440 vol.4.

[22] M. Shafi, M. Zhang, A. Moustakas, P. Smith, A. Molisch, F. Tufvesson, and S. Simon, "Polarized MIMO channels in 3-D: models, measurements and mutual information," *IEEE J. Sel. Areas Commun.*, vol. 24, no. 3, pp. 514–527, Mar. 2006.

[23] M. Coldrey, "Modeling and capacity of polarized MIMO channels," in *Proc. IEEE Veh. Technol. Conf.*, May 2008, pp. 440–444.

[24] C. Oestges, B. Clerckx, M. Guillaud, and M. Debbah, "Dual-polarized wireless communications: From propagation models to system performance evaluation," *IEEE Trans. Wireless Commun.*, vol. 7, no. 10, pp. 4019–4031, Oct. 2008.

[25] O. Özdogan and E. Björnson, "Massive MIMO with dual-polarized antennas," *IEEE Trans. Wirel. Commun.*, vol. 22, no. 2, pp. 1448–1463, Sep. 2023.

[26] A. S. de Sena, P. H. J. Nardelli, D. B. da Costa, P. Popovski, C. B. Papadias, and M. Debbah, "Dual-polarized massive MIMO-RSMA networks: Tackling imperfect SIC," *IEEE Trans. Wirel. Commun.*, vol. 22, no. 5, pp. 3194–3215, Oct. 2023.

[27] L. Sung, D. Park, and D.-H. Cho, "Limited feedback hybrid beamforming based on dual polarized array antenna," *IEEE Comm. Lett.*, vol. 22, no. 7, pp. 1486–1489, Mar. 2018.

[28] S.-C. Kwon and G. L. Stüber, "Polarization division multiple access on NLoS wide-band wireless fading channels," *IEEE Trans. Wirel. Commun.*, vol. 13, no. 7, pp. 3726–3737, Mar. 2014.

[29] S. Lee, H. Jo, C. Mun, and J.-G. Yook, "Implementation of polarization matching technique for polarization division multiple access," in *Proc. IEEE VTC-Spring*, Nov. 2017, pp. 1–5.

[30] S. Chatterjee, S. Dey, and R. Budhiraja, "Design and analysis of MMSE precoder for dual-polarized cell-free massive MIMO systems," *IEEE Commun. Lett.*, vol. 27, no. 10, pp. 2752–2756, Aug. 2023.

[31] J. Park and B. Clerckx, "Multi-user linear precoding for multi-polarized massive MIMO system under imperfect CSIT," *IEEE Trans. Wirel. Commun.*, vol. 14, no. 5, pp. 2532–2547, Jan. 2015.

[32] ——, "Multi-user linear precoding in massively distributed polarized antenna systems under imperfect CSIT," *IEEE Trans. Veh. Technol.*, vol. 69, no. 5, pp. 5268–5280, Mar. 2020.

[33] S. Gong, C. Xing, S. Chen, and Z. Fei, "Secure communications for dual-polarized MIMO systems," *IEEE Trans. Signal Process.*, vol. 65, no. 16, pp. 4177–4192, May 2017.

[34] M. R. Castellanos and R. W. Heath, "Linear polarization optimization for wideband MIMO systems with reconfigurable arrays," *IEEE Trans. Wirel. Commun.*, vol. 23, no. 3, pp. 2282–2295, Jul. 2024.

[35] Z. Chen, W. Wang, W. Zhang, T. Wan, and L. Liu, "Hybrid polarized beamforming optimization of millimeter wave multi-user massive MIMO communication systems," *IEEE Trans. Veh. Technol.*, pp. 1–11, Mar. 2025.

[36] P. Oh and S. Kwon, "Multipolarization superposition beamforming: Novel scheme of transmit power allocation and subcarrier assignment," *IEEE Trans. Wirel. Commun.*, vol. 22, no. 1, pp. 658–670, Aug. 2023.

[37] R. P. Antonioli, G. Fodor, P. Soldati, and T. F. Maciel, "User scheduling for sum-rate maximization under minimum rate constraints for the MIMO IBC," *IEEE Wirel. Commun. Lett.*, vol. 8, no. 6, pp. 1591–1595, Jul. 2019.

[38] J. Kaleva, A. Tölli, and M. Juntti, "Decentralized sum rate maximization with QoS constraints for interfering broadcast channel via successive convex approximation," *IEEE Trans. Signal Process.*, vol. 64, no. 11, pp. 2788–2802, Feb. 2016.

[39] J. Shi, A.-A. Lu, W. Zhong, X. Gao, and G. Y. Li, "Robust WMMSE precoder with deep learning design for massive MIMO," *IEEE Trans. Commun.*, vol. 71, no. 7, pp. 3963–3976, Apr. 2023.

[40] J. Fu, Z. Mobini, H. Q. Ngo, P. Zhu, and M. Matthaiou, "WMMSE-based processing in cell-free massive MIMO systems," *IEEE Wirel. Commun. Lett.*, vol. 14, no. 2, pp. 330–334, Nov. 2025.

[41] M. Grant, S. Boyd, and Y. Ye, "CVX: Matlab software for disciplined convex programming," 2008.

[42] S. K. Joshi, P. C. Weeraddana, M. Codreanu, and M. Latva-aho, "Weighted sum-rate maximization for MISO downlink cellular networks via branch and bound," *IEEE Trans. Signal Process.*, vol. 60, no. 4, pp. 2090–2095, Dec. 2012.

[43] S. P. Boyd and L. Vandenberghe, *Convex optimization*. Cambridge university press, 2004.

[44] X. Chen and C. Yuen, "On interference alignment with imperfect CSI: Characterizations of outage probability, ergodic rate and SER," *IEEE Trans. Veh. Technol.*, vol. 65, no. 1, pp. 47–58, Jan. 2016.

[45] J. Yao, Z. Yang, W. Xu, D. Niyato, and X. You, "Imperfect CSI: A key factor of uncertainty to over-the-air federated learning," *IEEE Wirel. Commun. Lett.*, vol. 12, no. 12, pp. 2273–2277, Sept. 2023.